SCIENCE-BASED RISK GOVERNANCE
OF NANO-TECHNOLOGY

RISK GONE

Report on pre-validated high throughput (*in vitro*) and miniaturised (*in vivo*) methods for ecotoxicity testing

DELIVERABLE 6.2

Due date of Deliverable:	31.12.2022
Actual Submission Date:	12.04.2023
Responsible partner:	HVL, Norway
Report Author(s):	Emil Cimpan, HVL, Iseult Lynch, UoB, Mihaela Cimpan, UiB, Ivan Rios-Mondragon, UiB, Håkon van Ta, UiB, Ole-Bendik Hofshagen, UiB
Reviewed by:	
Nature:	R (Document, report)
Dissemination Level:	PU (Public)

Call:	H2020-NMBP-13-2018
Topic:	Risk Governance of nanotechnology
Project Type:	Research & Innovation Action (RIA)
Name of Lead Beneficiary:	NILU, Norway
Project Start Date:	1 January 2019
Project Duration:	50-Months

This project has received funding from the European Union's Horizon 2020 research and innovation programme under grant agreement No 814425.

Document History

Version	Date	Authors/ who took action	Comment	Modifications made by
0.1	07-02-2023	Emil Cimpan (HVL)	First Draft sent to partners in the task	Mihaela Roxana Cimpan (UiB)
0.2	10-03-2023	Mihaela Roxana Cimpan (UiB)	Second Draft sent to partners in the task and coordinator	Maria Dusinska (NILU)
0.3	22-03-2023	PMO (NILU)	Third Draft sent to EAB and PMB	Iseult Lynch (UoB)
1.0	12-04-2023	PMO (NILU)	Submitted to Commission	

This project has received funding from the European Union's Horizon 2020 research and innovation programme under grant agreement No 814425.

Abstract

The aim of Task 6.2 was to refine *in vitro* models and mechanistically relevant high-throughput assays for nanosafety eco-toxicological hazard assessment and thus to speed up the transition towards a reliable, robust and cost-efficient replacement of *in vivo* testing. For this purpose, alternative *in vitro* assays, including impedance-based testing for both adherent cells and cells in suspension under static and dynamic exposure conditions and using a lab-on-a-chip biomimetic microfluidic platform coupled with live microscopy, were designed and implemented for nanotoxicity testing. Furthermore, cyclic voltammetry, an electrochemical method, was adapted for the first time for the assessment of engineered nanomaterials (ENM)-induced oxidative stress in a label-free manner and a mathematical model to interpret the results was developed.

In Task 6.2, we finalised *in vitro* assays based on rainbow trout gut and zebrafish embryo cell lines (UiB and UoB) and a *Daphnia magna* conditioned medium miniaturisation set-up that uses individual daphnids but replicates the population effects of multiple daphnids per vessel (UoB), using conditions that are more relevant for *in vivo* exposure to ENMs. One of the main sources of uncertainties in nanotoxicity assessment is represented by ENM interferences with testing systems. To address this, impedance-based methods that are label-free and thus, less prone to interferences were employed. Another important advantage of such methods is monitoring of cells in real-time, which allows the identification of relevant concentrations and timepoints for further in-depth mechanistic studies. Impedance-based monitoring gives information regarding cell proliferation, adhesion and viability and by coupling it with live microscopy, a more complete image of cellular behaviour during ENM exposure can be obtained. The biological models were exposed to a set of ENMs under static and dynamic exposure conditions, using the protocols established in WP4.

The data obtained, the methods and the biological models are also feeding into NanoHarmony for further evaluation and into inter-laboratory comparisons (ILCs), to support the activities of the OECD Working Party on Manufactured Nanomaterials (WPMN) and other standardization bodies. This activity forms the basis of Standard operating procedures (SOPs) to be taken forward as guidance documents to ensure the translation of the scientific data generated into risk management tools underpinning an environmental risk assessment (ERA) framework.

This project has received funding from the European Union's Horizon 2020 research and innovation programme under grant agreement No 814425.

TABLE OF CONTENTS

This project has received funding from the European Union's Horizon 2020 research and innovation programme under grant agreement No 814425.

This project has received funding from the European Union's Horizon 2020 research and innovation programme under grant agreement No 814425.

List of Abbreviations

2D	Two-dimensional
3Rs	Reduce, Replace, Refine (animal testing)
AA	Ascorbic acid
AC	alternating current
APS	Average particle size
BSA	Bovine serum albumin
CCM	Cell culture medium
CI	Cell index
CO_2	Carbon dioxide
CuO	Copper oxide
CV	Cyclic voltammetry
DLS	Dynamic light scattering
DMEM	Dulbecco's modified Eagle's medium
DMEM/F12	Dulbecco's modified Eagle's medium: Nutrient mixture F-12
DSE	Delivered sonication energy
EC	Effective concentration
EDTA	Ethylenediaminetetraacetic acid
ELS	Electrophoretic light scattering
ENM	Engineered nanomaterial
ERA	Environmental risk assessment
ERM	European Registry of Materials
EtOH	Ethanol
FBS	Foetal bovine serum
FC	Foldchange vs control
h	hour
HDD	Hydrodynamic diameter
HTS	High throughput screening
HVL	Western Norway University of Applied Sciences
ILC	Inter-laboratory comparison

This project has received funding from the European Union's Horizon 2020 research and innovation programme under grant agreement No 814425.

JRC	Joint Research Center
L15	Leibovitz' 15 cell culture medium
LIST	Luxembourg Institute of Science and Technology
LMWA	Low-molecular-weight antioxidant
min	Minutes
MWCNT	Multi-walled carbon nanotube
N_2	Nitrogen
NCI	Normalized cell index
NILU	Norwegian Institute for Air Research
OECD	Organization for Economic Cooperation and Development
PBS	Phosphate-buffered saline
PDI	Poly dispersity index
PDMS	Polydimethylsiloxane
PLL	Poly-L-lysine
PS	Penicillin Streptomycin
ROS	Reactive oxygen species
SOP	Standard operating procedure
TAC	Total antioxidant capacity
UA	Uric Acid
UiB	Bergen University
UoB	University of Birmingham
WC-co	Tungsten Carbide/Cobalt
WPMN	Working Party on Manufactured Nanomaterials
ZnO	Zinc Oxide
ZP	Zeta potential

This project has received funding from the European Union's Horizon 2020 research and innovation programme under grant agreement No 814425.

1. Introduction

This deliverable represents the outcome of the research and method validation undertaken in the context of RiskGONE Task 6.2 "*Refinement of innovative in vitro models and mechanistically relevant high-throughput assays for nanosafety eco-toxicological hazard assessment*". There is an urgent demand for reliable high-throughput testing systems to assess the toxicity of engineered nanomaterials (ENMs), both at an initial screening level and at a more in-depth mechanistic level due to the rapid development of new and more complex ENMs and their applications, which regulatory processes are struggling to keep pace with using traditional approaches.

The aim of this task was to provide *in vitro* assays that more realistically represent real-life exposure conditions yet are not overly complex in terms of interpreting the results, with the goal of driving progress towards the replacement of *in vivo* testing by alternative *in vitro* assays that are reliable, robust, cost- efficient and ecologically friendly.

The heterogeneity and increasing complexity of ENMs severely limit the feasibility of producing general toxicity protocols to address hazard assessment. Moreover, ENMs have been shown to often interfere with testing systems, which enhances the uncertainty regarding their biological effects (Kroll et al. 2012, Seiffert et al. 2012, Vinkovic et al. 2015). This leads to an increasing and urgent demand for reliable, robust and validated protocols for testing ENM toxicity, which are essential for the environmental, and implicitly human health-related hazard and risk assessment (Collins et al. 2016, Fadeel et al. 2018). So far, no consensus has been established regarding models and tests to assess the *in vitro* toxicity of ENMs and at present no clear regulatory guidelines on testing and evaluation are available (Drasler et al. 2017). For ecotoxicity testing, another ongoing challenge has been the large volumes of testing approaches and thus the high quantities of ENMs needed for such tests, which for low volume ENMs can be prohibitively expensive.

High throughput screening (HTS) techniques aimed at accurately assessing and predicting toxicity of large numbers of ENMs in a timely manner and with savings in labour costs and sample volumes are clearly needed. HTS is defined as the use of automated tools to facilitate rapid execution of a large number and variety of biological assays that may include several substances in each assay (Collins et al. 2016). HTS was introduced in the pharmaceutical and chemical industries as a rapid way of evaluating the effects of many novel compounds in parallel. Provided that reliable toxicity metrics have been established, the HTS approach can generate large and valuable data sets and facilitate the hazard ranking of ENMs, through the generation of database(s) with all reported effects on environmental systems. One of the main priorities in nanotoxicology is the development of new or adaptation of existing instruments and methods (Dusinska et al. 2015) that (i) recreate the biological environment and type of exposure to ENMs to increase the *in vivo* relevance of HTS and (ii) are not distorted by ENM-caused interferences with assay components and/or testing systems (Guadagnini et al. 2015). Some of the most encountered interferences are with fluorescent markers, which could be adsorbed onto ENMs preventing the markers from being available to bind to cellular structures of interest. In some cases, ENMs fluoresce themselves and/or are able to act as fluorescence quenchers. Moreover, a general drawback of fluorescence-based assays is that a good quantification of fluorescence is difficult to obtain.

During handling through multiple steps in traditional toxicity assays cells can become permanently modified and damaged. Such assays are often time-consuming, labour-intensive, and complex (Ceriotti et al. 2007). Another drawback of many traditional methods is that they can only evidence effects at a specific point in time and thus do not give an overview of the biokinetic behaviour and of the real-time

This project has received funding from the European Union's Horizon 2020 research and innovation programme under grant agreement No 814425.

interactions between biological structures and toxicants over time (Ceriotti et al. 2007). The need for label-free detection methods has therefore emerged, especially in nanotoxicity studies.

This aim of increasing throughput, reducing volume of ENMs required and providing label-free assays has been accomplished by finalizing *in vitro* assays based on fish cell lines, i.e., Rainbow trout intestinal cells (RTgut) (UiB) and 1-day old embryonic zebra fish cells (ZF4) cells (UiB and UoB), as well as through optimization of a conditioning medium protocol coupled with a miniaturized assay for *Daphnia magna* (*D. magna*) acute toxicity that can be performed in a 24-well or 48-well plates, developed at UoB. For the initial high-throughput toxicity screening, the electrical impedance-based monitoring of cells, that allows for real-time and label-free cell tracking while minimizing the possibility of ENM interference, was employed (Cimpan et al. 2013). The electrical impedance method uses the electrical characteristics of cells to monitor cellular behavior continuously over longer time intervals, up to two weeks. Because most mammals are either primary or secondary consumers of aquatic species, ecotoxicological experiments utilizing fish models could be useful for combining toxicological testing of mammalian models. Moreover, using continuous fish cell cultures instead of fish proves to be cost- and time-efficient, as well as being compliant with the 3Rs Directive (Directive 2010/63/EU) to Replace, Reduce and Refine animal studies, since the continuous cell lines don't require animal husbandry.

The impedance-based screening is time efficient and does not require chemical reagents. Furthermore, a microfluidic-chip impedance-based system combined with live-imaging was developed to mimic the dynamic *in vivo* exposure to ENM dispersions (Ruzycka et al. 2019). To assess oxidative stress in a label-free manner, UiB has established cyclic voltammetry (CV) for nanotoxicity testing using human lung cancer A549 epithelial cells in WP5 and will also be implemented for fish cells. Mathematical models were developed to interpret the results of CV and of impedance-based testing on adherent cells, the latter incorporating the kinetics of cellular response to ENMs (HVL).

The ENMs were dispersed following the SOPs developed in WP4, as well as the NANOGENTOX protocol for a subset of ENMs. The Hydrodynamic diameter was measured at the beginning and end of exposure using the Dynamic light scattering (DLS) method.

The miniaturized daphnia assay using conditioned medium is an extension of the published work performed in the context of the FP7 project FutureNanoNeeds to systematically evaluate the impacts of varying total medium volume, surface to volume ratio and animal density for the acute toxicity testing of chemicals (Grintzalis et al., 2017), utilizing immobilization as a surrogate measure of their mortality (as per the OECD acute toxicity test 202) and feeding rate, which in Daphnia is determined by measuring the algae feeding rate. 6-24 Within RiskGONE we assessed the applicability also for ENMs, and given that ENMs are known to form an eco-corona and to require biomolecules to stabilize them, we also included a conditioning step whereby the medium used to disperse the particles is pre-exposed to daphnid neonates for a specific period prior to ENM dispersion, thus conditioning the medium by secreting proteins and other biomolecules into the medium. Use of conditioned medium also has benefits for the daphnids, especially in further adapting the miniaturized assays for chronic studies, since Daphnia are well-known to secreted signalling molecules called kairomones to communicate with one another, and within RiskGONE we have demonstrated that Daphnia lifespan is significantly reduced when daphnids are cultured singly rather than in groups, but that the longevity can be almost fully restored by culturing the daphnids singly but in conditioned medium (see Nasser et al., 2020).

This project has received funding from the European Union's Horizon 2020 research and innovation programme under grant agreement No 814425.

2. Background information

Impedance-based assays that measure the electrical properties of cells are label-free and represent a reliable alternative with the potential to become a method of choice for the initial screening of ENMs' toxic effects. They take advantage of the passive properties of an object, which occur when the object is composed of dissipative elements, such as ohmic resistors or conservative elements such as capacitances and inductances. Impedance-based assays measure how much objects, such as cells, impede a flow of electrical current. Proliferation, growth, morphology, and adhesion can be measured by applying an electric source to an electrode covered by cells, and measuring how the cells impede the current. By using alternating current (AC), information about the properties of the cells as a function of signal frequency is obtained. Cell membranes are insulating structures with an abundance of negatively charged molecules on the inside as compared to the outside, which gives rise to the resting potential of the membrane. When a time-oscillating electric field is applied, a change in the charge distribution will ensue, with charged molecules trying to follow the electric field. The polarisation effect depends on frequency and gives rise to α-, β- and γ dielectric dispersions (Pliquett 2010) (Fig. 1).

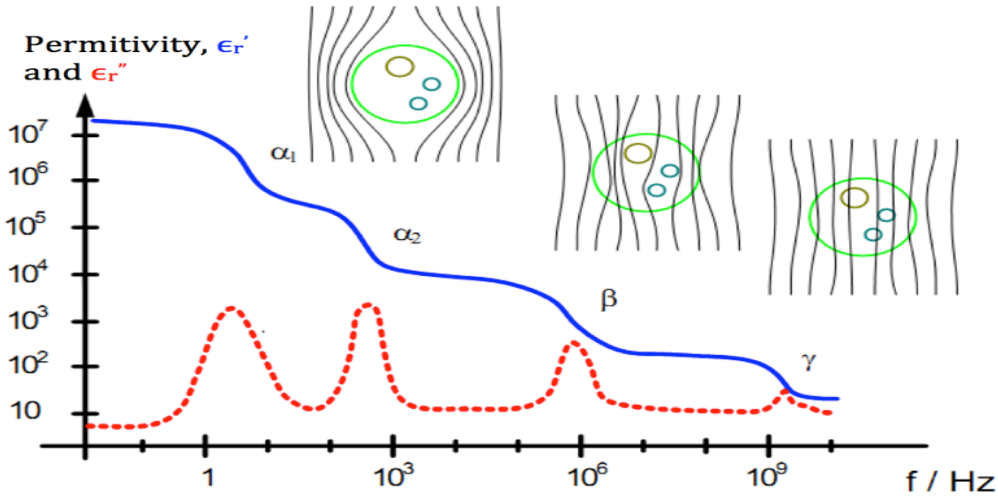

Fig. 1. Dispersion types. The higher frequencies allow easier passage of current through the cell. The real dielectric number ϵ_r' is shown in blue, while the imaginary part ϵ_r'' is shown in red. α -dispersion has an active cell-membrane effect. In β-dispersion, the passive cell membrane-capacitance is observed. The γ-dispersion is due to polarization of the medium in the cell (water, salts, proteins). Figure adapted by Pliquett from Schwan and Kay (1957).

For a cell placed between two electrodes, there is a relationship between the different dispersions and the polarisation of the cell (Fig. 2). At low frequencies, a lateral movement of ions along insulating membranes takes place, giving rise to α-dispersion. As a result, a high polarisation of the membrane is obtained together with a high permittivity. Impedance measurement at low frequencies gives information about the size of the cell (Cheung et al. 2010). When frequency is increased, the charged molecules cannot follow the electric field anymore, because of its rapid fluctuation, leading to a decrease in the capacitance of the membrane. Between 100 kHz and 10 MHz the rapid depolarisation, known as β-dispersion, can be observed and measurements within this range can give information about membrane properties (Prodan et al. 2008, Pliquett 2010). At very high frequencies (1GHz), γ-dispersion occurs as a result of the polarisation of water, salts and proteins in the cell.

This project has received funding from the European Union's Horizon 2020 research and innovation programme under grant agreement No 814425.

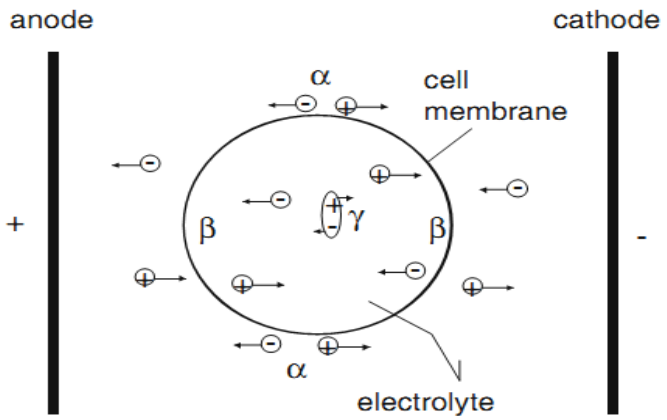

Fig. 2. Polarisation mechanisms for a cell situated between two electrodes. Movement of ions along the cell membrane gives α-dispersion. β-dispersion occurs as the cell membrane is depolarised. γ-dispersion is recognised due to polarisation of macromolecules (Pliquett, 2010).

Impedance-based methods have an advantage when compared to traditional methods because they allow "*in situ*" real-time recordings without the use of markers, as well as enabling monitoring of the dynamics in cell growth and viability (Hondroulis et al. 2010). The xCELLigence system (Agilent Technologies, Santa Clara, CA, USA) was used in WP6 to monitor the effects of ENMs on adherent cells (UiB). For cells in suspension, the microfluidic chip-based impedance flow cytometer Ampha Z30 (Amphasys AG) has been introduced by UiB for nanotoxicity testing in human cells in suspension (Ostermann et al. 2020), who is currently implementing it for testing on fish cells. Furthermore, microfluidic impedance-based biomimetic chips have been designed and produced (UiB) for testing and recording of ENM effects on ZF4 cells in real-time under dynamic exposure and the system is currently being optimised.

To assess the putative oxidative stress induced by ENMs, CV was implemented in WP5 and is also being applied to fish cells (UiB). CV is a label-free method, which can be used to assess the redox-properties of biofluids by applying an electrical potential in a cyclic manner and measuring the resulting current as electrons are transferred in a redox (reduction-oxidation) reaction. Because most low-molecular-weight antioxidants (LMWAs) are reducing agents that scavenge reactive oxygen species (ROS) and quench them by electron donation, measuring a sample's total reducing power by CV can reveal the LMWA activity in the sample (Chevion et al. 2000). The oxidative scan is crucial for evaluating the total antioxidant capacity (TAC) because it gives critical details about the antioxidant content of the sample. As it can be seen in Figure 3, the anodic peak current, $i_{pa,}$ describes the antioxidant's reducing power, and the anodic peak potential, E_{pa}, characterizes the specific antioxidant measured. Together, these measured parameters provide information on what antioxidants are present, their inherent capacity of reducing other substances, and their concentrations. The i_{pa} increases linearly with concentration and can thus, be used to estimate the antioxidant concentration (Psotova et al. 2001). The resulting micro-scale currents make it possible to track even minute changes in antioxidant capacity. When a voltage is applied to the working electrode, it becomes sufficiently positive or negative to oxidise or reduce the molecule of interest. In the case of an oxidative scan, the current increases until it reaches the i_{pa}, then decreases as the reduced state of the molecule of interest depletes at the anodic surface.

This project has received funding from the European Union's Horizon 2020 research and innovation programme under grant agreement No 814425.

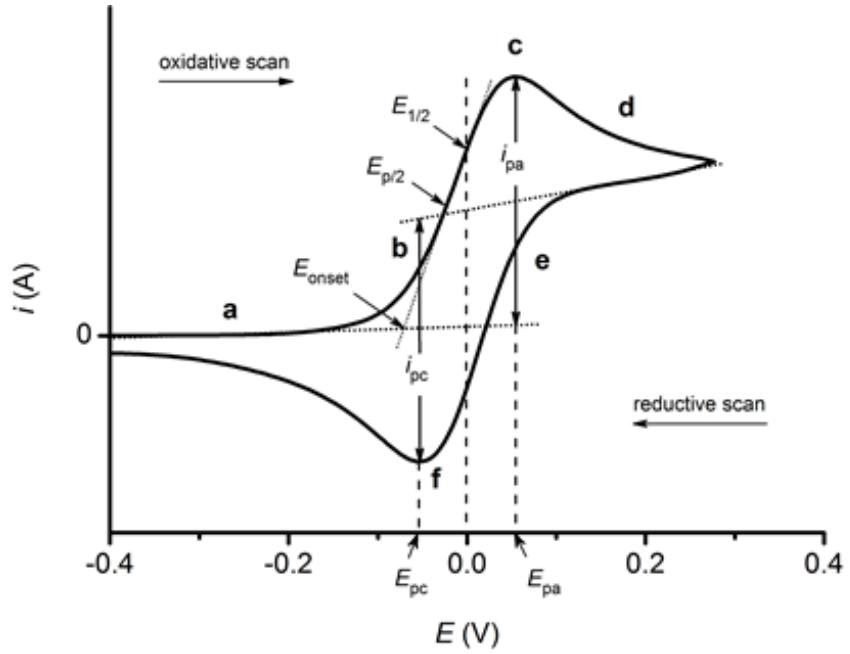

Fig. 3. Typical cyclic voltammogram where i_{pc} and i_{pa} show the cathodic and anodic peak current, respectively. E_{pc} and E_{pa} show the cathodic and anodic peak potential, respectively.

A cyclic voltammogram's oxidative scan is heavily reliant on the antioxidants present in the sample, as they donate electrons at their oxidation potential. As a result, the integrated value of the oxidative scan can be presented as the sample's total antioxidant capacity. This method of evaluating antioxidant capacity, however, does not determine which specific antioxidants are present. Various antioxidants can be distinguished by the anodic peak potential at which they are oxidised. The potency of the antioxidants determines the potential for oxidation. For example, ascorbic acid (AA) is a more effective antioxidant than uric acid (UA) and is oxidised at a potential that is about 40 mV lower than UA (Chevion et al. 1997). In more complex biological samples where several antioxidants may contribute to the overall current, it has been proposed that the TAC may prove more useful when monitoring changes in antioxidant content than I_{pa} (Chevion et al. 1999). Because antioxidants are depleted during oxidative stress and CV is very sensitive to changes in antioxidant concentration, this approach has been demonstrated to be capable of tracking oxidative stress (Chevion et al. 1997). For electrochemically reversible couples when both the oxidized and reduced form is stable in solution and does not readily react with other species and can therefore be oxidized/reduced to its original state, the redox potential (E°) for the couple is the midpoint between E_{pc} and E_{pa}. Figure 4 shows a schematic representation of a traditional electrochemical cell and a commercial screen-printed electrode. CV typically employs a three-electrode configuration: the working, counter and reference electrodes. The oxidation/reduction reaction takes place at the working electrode. A potentiostat is used to apply a working electrode potential that is a function of the reference electrode potential. The working electrode's most significant properties are that it is inert to redox reactions and that it has a clean surface. The purpose of the reference electrode is to have a stable and well-defined equilibrium potential. This is extremely valuable since it serves as a reference against which the other electrodes are measured. Silver wires fed into a glass tube filled with electrolyte solution are commonly used as a reference electrode. The electrical current begins to flow when a voltage is provided to the working electrode and a redox reaction occurs. The counter electrode completes the circuit, allowing the current to be measured (Elgrishi et al. 2018).

This project has received funding from the European Union's Horizon 2020 research and innovation programme under grant agreement No 814425.

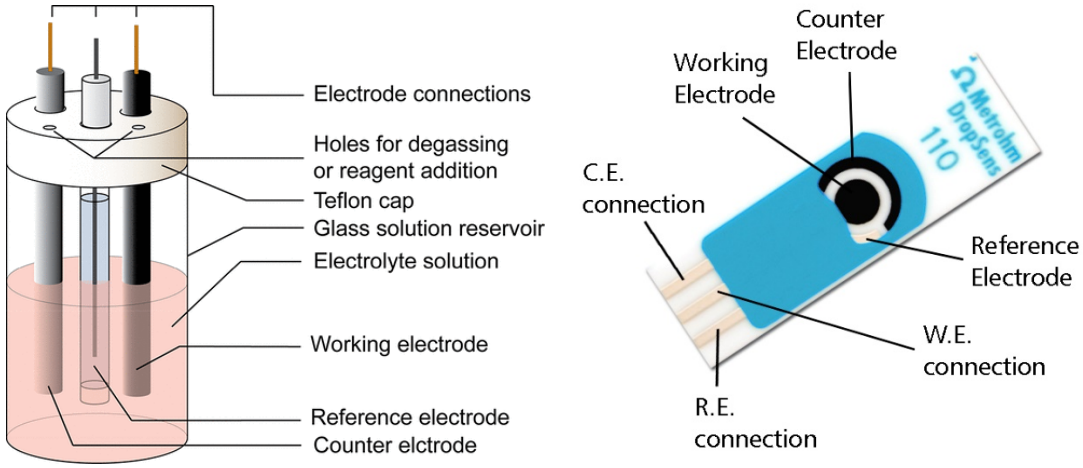

Fig. 4. Traditional electrochemical cell (left) and commerical screen printed electrode (right).

Eco-corona formation is a well-established process by which ENMs, which have a very high surface reactivity, are transformed once in contact with biological environments. Thus, ENM adsorb some of the biomolecules present in their surroundings onto their surface in order to try to reduce their surface reactivity. Which biomolecules from the available ones present in the particular environment bind to the ENM depends on both the biomolecule abundance and the affinity for the ENM surface, as well as the ENM characteristics (Lynch et al., 2014). Biomolecule binding to the ENM surface is driven by a range of forces including electrostatic, hydrophobic, entropic due to release of water or small ions, and indeed, some molecules may not bind directly to the ENM surface, but instead bind to other biomolecules or metabolites present in the eco-corona, as shown schematically in Figure 5 (Chetwynd et al., 2020). Initially proteins which are higher in abundance bind to NM surfaces and then are displaced by less abundant yet higher affinity proteins, as explained by the Vroman effect. Similarly, it has been shown that different environmental species are able to adsorb and displace others on the surface of 20 nm TiO_2 NMs, where humic acid adsorbs tightly to NM surfaces to form part of the eco-corona while smaller acidic molecules such as ascorbic and citric acid bind weakly and can easily be displaced by humic acid (Wu et al., 2019).

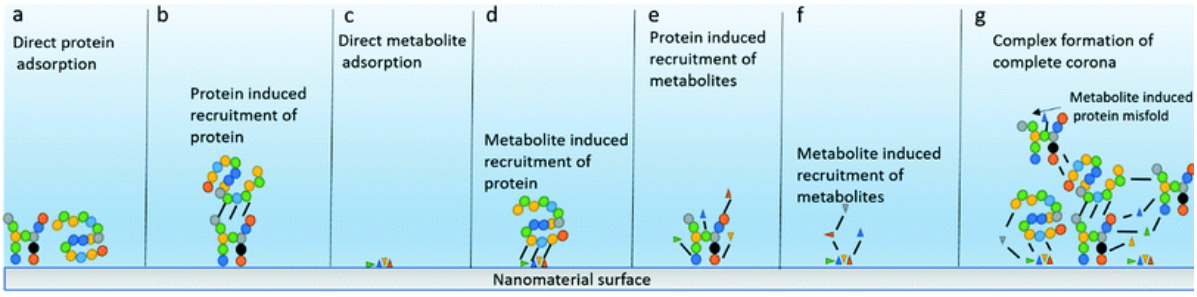

Fig. 5. Schematic illustration of hypothetical mechanisms for formation of the complete corona around ENMs. A wide range of possibilities exist for the corona to acquire metabolites and proteins. (a) The direct adsorption of proteins from the environment is the predominant model at the moment, however protein–protein interactions (b), metabolite adsorption (c), metabolite induced adsorption of proteins (d), protein induced recruitment of metabolites (e), metabolite induced recruitment of further

This project has received funding from the European Union's Horizon 2020 research and innovation programme under grant agreement No 814425.

metabolites (f) or more likely a complex combination of all aforementioned methods with elements such as metabolite induced conformational changes in proteins (g).

Medium conditioning is a key step recommended by RiskGONE in ENM ecotoxicity assays to begin to replicate the realistic environmental exposure conditions. For example, freshwaters in which Daphnia exist, will inevitably contain a vast array of biomolecules arising from runoff from vegetation resulting in the deposition of proteins, polysaccharides, and lipids within these waters, which are utilized for their amino-acids, monosaccharides, and fatty acids by organisms to support growth and development. A range of organisms, from the simplest bacteria to complex biofilms and aquatic dwelling plants and animals secrete biomolecules into their surrounding medium. These secretions are collectively known as "conditioning" of the medium and are an important source of biomolecules to the surrounding environmental waters. Organisms such as *D. magna,* which are a filter feeder, condition their surroundings by releasing substances called kairomones which trigger defence mechanisms in their prey such hat the organisms themselves are continually altering the concentrations of biological matter in their environment (Figure 6) (Nasser et al., 2020). *D. magna* also release proteins into their environment, for example, enzymes such as chitinase and chitinobase. These degrade the polymer chitin, which is the main component of the exoskeleton of *D. magna*, and are abundant prior to moulting, and released along with the moulting fluid into environmental waters. Polysaccharides are also secreted by *D. magna* into their surrounding environment as a natural process of growth and development, whereby the chitin-based exoskeleton is released into the surrounding water (Nasser et al., 2020).

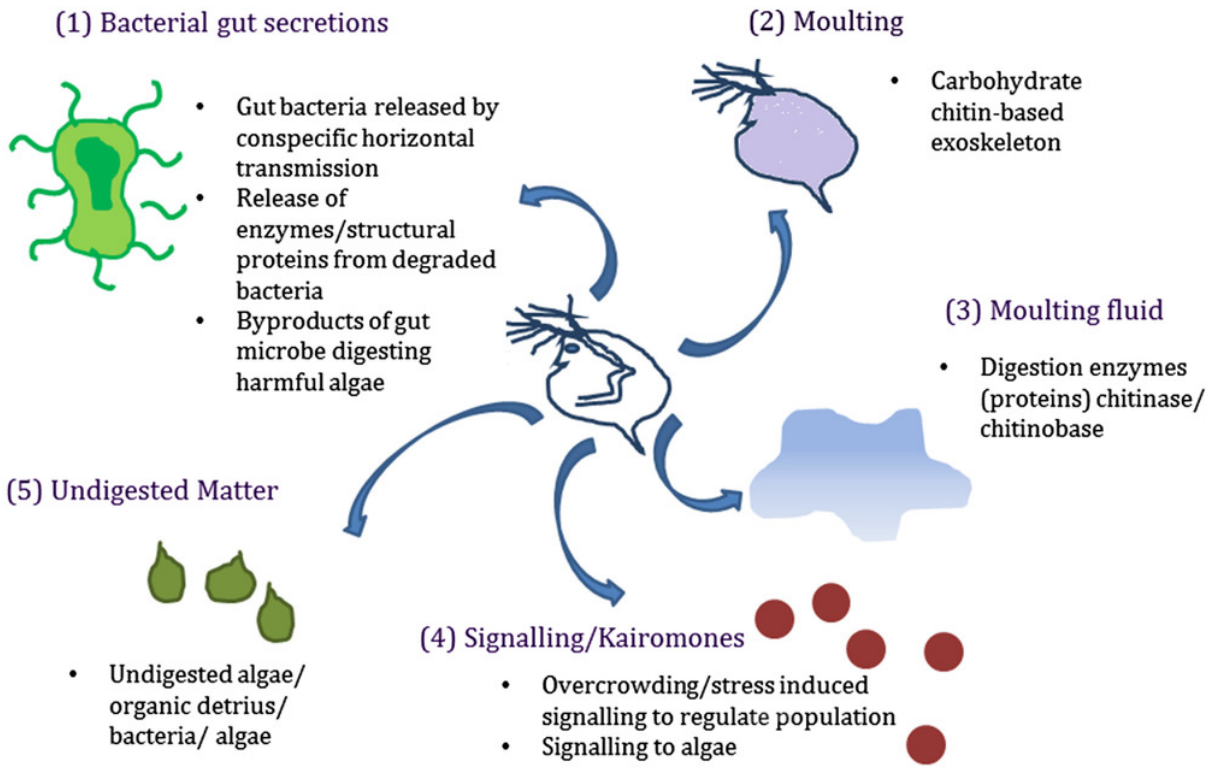

Fig. 6. Various secretions from *D. magna* including: 1) bacterial gut secretions, 2) carapace from moulting, 3) moulting fluid, 4) surface-based secretions and 5) undigested or partially digested matter. From (Nasser et al., 2020).

This project has received funding from the European Union's Horizon 2020 research and innovation programme under grant agreement No 814425.

3. Methodology

3.1 Impedance-based high-throughput testing of ENM toxicity on adherent cells

3.1.1 Cell culture

Two cell lines were used: Rainbow trout intestinal cells (RTgut) and 1-day old embryonic zebra fish cells (ZF4). Frozen cells were thawed, suspended in complete culture medium (CCM) and centrifuged at 1200 rpm for 5 min. The supernatant was removed, and the cells were resuspended in CCM and seeded in T75 culture flasks (ThermoFisher, Waltham, MA, USA). The cells were then transferred to incubators. The RTgut cells were provided by the Institute of Environmental and Water Research (Eawag, Switzerland) and the work was carried out at the Institute for Marine Research (Bergen, Norway). The ZF4 cells and the protocol for growing them were kindly provided by Prof. Iseult Lynch and Associate Prof. Zhiling Guo from the University of Birmingham (Birmingham, England). Table 1 summarizes the CCM and culture parameters for each cell line.

Table 1: Description of the characteristics and culture parameters of the cell lines used in testing.

Cell type	**Cell culture medium (10% FBS, 1% P/S)**	**Incubator - temperature and CO_2**	**Cell density at seeding (cells/cm^2)**
Rainbow trout intestinal cells (RTgut)	Leibovitz-15 (L15)	19°C, 0% CO_2	50.000
Zebrafish embryonic fibroblast cells (ZF4)	Dublecco's modified eagle medium: nutrient mixture F-12 (DMEM/F-12)	28°C, 5% CO_2	40.000

The cells were cultured in T75 vented treaded flasks with bent necks (Nunc, Roskilde, Denmark) in an incubator with the required temperature and CO_2 parameters for each cell line. The CCM was supplemented with 10% fetal bovine serum (FBS, Sigma-Aldrich) and 1% penicillin-streptomycin (P/s, Sigma-Aldrich). Fresh medium was given every 3 days and the cells were passaged at approximately 80% confluency by trypsinization. When 80% confluency was reached, the flask was washed twice with phosphate buffered saline (PBS) before adding 2 mL of trypsin-verse EDTA (Sigma-Aldrich). The cells were incubated for 5 min before the cell suspension was mixed with 8 mL of CCM, then transferred to a 15 mL tube, which was centrifuged at 1200 rpm for 5 min. The supernatant was discarded and afterwards the cell pellet was resuspended in 10 mL CCM. The cells were stained with trypan blue for viability assessment and counted using an Invitrogen Countess II automated cell counter (ThermoFisher, Waltham, MA, USA). A volume of 10 µL of trypan-blue 0.4% (ThermoFisher, Waltham, MA, USA) and 10 µL of cell suspension were placed in a 500 µL Eppendorf tube and thoroughly mixed. Out of the mixture, 10 µL were pipetted to both chambers of an Invitrogen Countess chamber. The automatic cell counter was then used to count cell viability and cell amount. Only cells in passage 4-15 with viability above 90% were used in experiments.

This project has received funding from the European Union's Horizon 2020 research and innovation programme under grant agreement No 814425.

3.1.2 Daphnia culturing and medium conditioning

Initial stocks of *D. magna* were maintained using pools of 3rd brood Bham2 strain (genetically identical), which originated from the University of Reading and the Water Research Centre, Medmenham, UK. *D. magna* were kept in a 20 ºC temperature-controlled environment with 12-hour light and dark cycles. *D. magna* were cultured in a standard high hardness *Daphnia* culturing media 67 and the artificial river water representative 68 which was refreshed weekly to ensure healthy culture maintenance. *D. magna* cultures were fed Chlorella vulgaris algae daily, to a total of 0.5 mg carbon between days 0-7 (750 µL) and 0.75 mg (1.5 mL) carbon from day 7.

To condition medium by *D. magna*, 10 neonates (1–3 days old) were placed in 5 mL of HH Combo medium and were allowed to condition the medium for a specified conditioning time. Conditioning time starts when neonates are put into HH Combo medium and allowed to secrete proteins for a given length of 'conditioning time' (1, 3 or 6 h) whereby they are then removed from the medium leaving behind only medium with the secreted proteins (conditioning time for medium). Neonates were not fed in order to ensure the proteins and other biomolecules accumulated in the medium were only released by the neonates themselves, albeit including their gut microbiome. At the end of the conditioning time neonates were carefully pipetted out of the medium leaving only the remaining conditioned medium.

3.1.3 Nanomaterials and dispersion protocols

Six different types of ENMs were used. Four of the six particles were supplied as powders and dispersions of these were prepared following the NANOGENOTOX protocol (Jensen et al. 2011) and the DeLoid-protocol (DeLoid 2017), as specified in Table 2. Multi-walled carbon nanotubes (MWCNT, Nanocyl) and ZnO ENMs (Sigma-Aldrich) were provided as dispersions in water-based medium and for these only vortexing was used for dispersion. A 130-Watt probe sonicator (VCX130, Vibra-Cell, 130W, Sonic & Materials, Newtown, USA) was used at 22% amplitude of the maximum amplitude, equipped with a 12.8 mm probe with a replaceable tip to prepare particle dispersions. The sonicator was calibrated to ensure that the desired energy was delivered to the systems. The power (P) was found to be 6.1919 J for the DeLoid-protocol and 8.41 J for the NANOGENOTOX-protocol. By implementing the referenced critical delivered sonication energy (DSE_{cr}) (see Table 2) and Equation 1 the sonication time (t_{cr}) needed to disperse the ENMs was calculated.

$$t_{cr} = \frac{DSE_{cr}}{P} V \qquad (1)$$

where t_{cr} = critical sonication time (s), DSE_{cr} = Referenced delivered sonication energy (J/mL), P = Sonicator power (J/s) and V = Volume of dispersion (mL).

This project has received funding from the European Union's Horizon 2020 research and innovation programme under grant agreement No 814425.

Table 2: The ENMs and dispersion protocols used in Task 6.2

Particle (ERM identifier)	Dispersion protocol	Description (supplier code)	Nominal size	Stock concentration (mg/mL)	Reference DSE_{cr} for sonication (J/mL)
CuO (ERM00000088)	Sonication - DeLoid	PlasmaChem (PL-CuO)	Ca. 40 nm (APS)	5	40.18
WC-co (ERM00000089)	Sonication - Nanogenotox	NanoAmor (5561HW)	<200 nm (APS)	2.56	3.136
MWCNT (ERM00000325)	Vortexing	Nanocyl (AQUACYL™, AQ0303)	Average diameter, 9.5 nm. Average length, 1.5 µm.	5	-
TiO2 (ERM00000064)	Sonication - DeLoid	JRC (JRCNM01005a)	15-24 nm (TEM)	5	322.32
TiO2 (ERM00000062)	Sonication - DeLoid	Sigma-Aldrich (637254)	<25 nm (APS)	5	193
ZnO (ERM00000063)	Vortexing	Sigma-Aldrich (721077)	<100 nm (TEM), ≤40 nm (APS)	240	-

APS: Average particle size.

DeLoid-protocol

A mass of 15 mg of ENM raw material was carefully weighted in a 20 mL scintillation vial by using a disposable plastic antistatic spatula. MilliQ water was added drop-by-drop to the glass scintillation vial while tilting and swirling the vial, so that a concentration of 5 mg/mL was reached. After swirling the vial containing ENM and milliQ water, the mixture sonication could begin. Without touching the sides of the vial, the tip of the sonicator probe was placed inside the vial. The tip was submerged at 2/3 of the height of the vial carefully, not touching the bottom. The ENM was then sonicated according to the DSE_{cr}-values specified in the LIST-protocol. The amount of time calculated as necessary to sonicate the dispersion was 19 sec for CuO, 93,5 sec for TiO_2 (Sigma-Aldrich) and 156,2 sec for TiO_2 (JRC). To protect it against light, the dispersion was sealed and covered with aluminum foil.

NANOGENOTOX-protocol

A mass of 15.36 mg of ENM raw material was weighed in a 20 mL scintillation vial by using a disposable plastic antistatic spatula. The vial was tilted at a 45° angle and tapped gently on the side to gather the material. A volume of 30 µL EtOH (96%) was added drop-by-drop onto the raw material and mixed gently. A volume of 970 µL of 0.05% BSA water was added slowly to avoid foaming. Lastly, an additional 5 mL of 0.05% BSA water was added slowly along the walls of the vial to collect any powder that might have deposited on the walls. A stock concentration 2.56 mg/mL was made. The vial was sealed with a cap and placed on ice for at least 5 min, while the sonicator was prepared. The sonicator probe was carefully submerged in the scintillation so that to avoid touching any of the sides. The ENM dispersion

This project has received funding from the European Union's Horizon 2020 research and innovation programme under grant agreement No 814425.

was sonicated according to the DSE_{cr}-values specified in the NANOGENOTOX-protocol. The time calculated to sonicate the WC-Co dispersion was 2 sec. Afterwards, the dispersion was sealed with a cap and covered with aluminum foil and placed on ice to rest.

Multi-Walled Carbon Nano Tubes (AQUACYL 3 wt. % NC7000*)*

The MWCNT (AQUACYL 3 wt. % NC7000) were provided by Nanocyl (Sambreville, Belgium). The MWCNT (AQUACYL 3 wt. % NC7000) dispersion was a pitch-black dense viscous solution, which was vortexed vigorously for 30 sec. An intermediate suspension was made by extracting a quantity of 1 mL of stock dispersion and diluting it at 1:6 ration in the proprietary dispersant (1 mL AQUACYL 3 wt.% dispersion + 5 mL Dispersant). Thus, a concentration of 5 mg/mL was obtained.

Zinc Oxide (ZnO)

ZnO was provided by Sigma-Aldrich (Darmstadt, Germany). The density of the ZnO bottled in suspension was estimated at 240 mg/mL.

Preparation of ENM dispersions in cell culture medium

The ENM was dispersed in a 15 mL tube cell culture medium at required concentrations by adding fresh vortexed ENM dispersions to complete the cell culture medium. The tube with the solution was then rotated in the tube rotator ISB3 (Bibby Scientific, Staffordshire, England) at 40 rpm for 2 minutes and mixed with a pipet. When multiple concentrations were prepared, a high concentration tube (100 µg/mL or 50 µg/cm^2) was used for serial dilution. In each dilution series step, the solution was mixed by pipet and vortexed for 5 seconds. Before exposure to cells, the solution was mixed with pipet.

3.1.4 Nanoparticle characterization

Dynamic light scattering

DLS using a Zetasizer Nano ZSP (Malvern Instruments, Malvern, England) was employed to evaluate the size of the batch dispersions and of ENMs in complete cell culture medium. For the latter, the highest exposure concentration (100 µg/mL) was used. Three measurements of the hydrodynamic diameter (HDD) and polydispersity index (PDI) were performed for each sample at the beginning and end of exposure to ENMs.

Zeta potential

The Zeta potential (ZP) was measured for the ENMs dispersed in the two different CCMs. The CCMs were supplemented with 10% FBS and 1% P/S. In a prewetted folded capillary zeta cell (DTS1070, Malvern Instrument), 800 µL of the highest ENM concentration used in experiments (100 µg/mL which corresponds to 50 µg/cm²) was pipetted. The ZP was measured using a Zetasizer Nano ZSP at the temperature corresponding to that used during ENM exposure in the toxicity tests.

3.1.5 The 96-well E-plate preparation and treatment

The xCELLigence 96-well E-plates were used for impedance-based measurements of RTgut- and ZF4-cells. The preparation of the E-plate started by filling the sides around each well with sterile water before placing it in the incubator, to maintain humidity while the plate was sitting inside the incubator. Then,

This project has received funding from the European Union's Horizon 2020 research and innovation programme under grant agreement No 814425.

100 µL of fresh cell culture medium was pipetted into each well. The E-plate containing cell culture medium was kept at room temperature for 30 min before a background measurement was taken with the xCELLigence RTCA SP (ACEA Bioscience) inside the incubator. After this, the RTgut cells were seeded at 50.000 cells/cm² (10.000 cells/well) and the ZF4 cells at 40.000 cells/cm^2 (8.000 cells/well) in a total volume of 200 µL of cell culture medium. The plate was then placed in the xCELLigence system (ACEA Bioscience) and the impedance was measured for a 24 h period. After the 24 h period, the E-plate was removed from the xCELLigence system and 100 µL of cell culture medium were taken out from each well. In the wells with medium only (without cells) and the control group (unexposed cells) 100 µL of fresh complete medium were added. To identify possible ENM interferences, in a set of wells with medium only (without cells), 100 µL of the highest ENM concentration (50 µg/cm² corresponding to 100 µg/mL) were added. In the wells with cells, 100 µL of ENM dispersions in 5 different concentrations were added. The final exposure concentrations were: 1, 2, 5, 10, 25 and 50 µg/cm² (corresponding to 2, 10, 20, 50, and 100 µg/mL). Note that the added ENM dispersion concentration was x2 due to adding one half of the total volume of the well. The software displayed the *C,* based on impedance measurements, at every 15 min both before and after exposure, fora total of 48 h. Figure 7 displays the 96 E-plate layout used in experiments.

	1	2	3	4	5	6	7	8	9	10	11	12
A	M	M	M	M	M	M	M	M	M	2	2	2
B	M+100	M+100	M+100	M+100	M+100	M+100	M+100	M+100	M+100	2	2	2
C	C	C	C	C	C	C	C	C	C	2	2	2
D	20	20	20	20	20	20	20	20	20	10	10	10
E	50	50	50	50	50	50	50	50	50	10	10	10
F	100	100	100	100	100	100	100	100	100	10	10	10
G	M	M	M	M	M	M	M	M	M	M	M	M
H	M	M	M	M	M	M	M	M	M	M	M	M

NM1 in L15 only (100 µg/mL)	NM2 in L15 only (100 µg/mL)	NM3 in L15 only (100 µg/mL)
M: L15 medium only (no cell)	C: cells only (control)	
X: cells + NM1 at concentration X	X: cells + NM2 at concentration X	X: cells + NM3 at concentration X

Fig. 7. The 96-well plate layout showing the content of the wells: M = cell culture medium, C = control (unexposed cells), the numbers 2, 10, 20, 50, and 100 represent the ENM concentrations in µg/mL. Three ENMs could be tested in one plate on one type of cell, in the example above, on RTgut cells.

3.1.6 Impedance-based toxicity testing using the xCELLIgence system

The impedance-based measurements were performed using an xCELLigence RTCA SP instrument (Agilent, Santa Catalina, CA, USA) equipped with 96-wells for label-free, real-time monitoring of cell proliferation, adherence, and viability under static exposure conditions. The impedance at the gold-plated electrodes that covered 70-80% of the bottom of the wells on which the cells were seeded was recorded at a 15 min interval from cell seeding until the end of the exposure to ENMs. The experiments comprised three main steps: equilibration of the E-plate, seeding of cells and exposure of cells to ENMs. All experiments were done in duplicates or triplicates in three independent repetitions. The mean of the

This project has received funding from the European Union's Horizon 2020 research and innovation programme under grant agreement No 814425.

duplicates or triplicates was used to calculate the cell index (*CI*). The RTgut and ZF4 cells were exposed to ENMs after an initial cell seeding and proliferation for 24 h in the E-plates. In each experiment, the cells were seeded at the starting point and left to attach to the electrode surface and proliferate for 24 h before being exposed for 24 h to five different concentrations of ENMs: 2, 10, 20, 50, 100 µg/ml. The *CI*s were normalized to the *CI*-value measured right before the cells' exposure to the ENMs, i.e., at 24 h after seeding (Equation 2).

$$NCI = \frac{CI_t - CI_{med}}{CI_{t=24}} \qquad (2)$$

NCI = Normalized cell index

CI_t = Cell Index at timepoint *t* of exposure to ENM

CI_{med} = Cell index of the referenced medium, without cells

$CI_{t=24}$ = Cell index at timepoint 24 h (last timepoint before exposure to ENM)

For the control groups, the CI_{med} value that was chosen was the one for the cell culture medium alone (without cells), while for the exposed cells, the chosen CI_{med} value was the one for the medium with the highest concentration of ENMs, without cells. This was done to check for possible background interference from the ENMs. The normalized cell index (*NCI)* gives real-time information on cellular proliferation and viability of cells.

The fold-change vs control (*FC*) describes the ratio between the *CI* of the cells exposed to ENMs and the *CI* of the control (unexposed cells). The *FC* was calculated for the cells at 48 h after seeding i.e., at 24 h after exposure to ENMs (Equation 3). An *FC* > 1 indicated increase of cellular proliferation and viability compared to the control, and an *FC* < 1 indicated a decrease of proliferation and non-viability.

$$FC = \frac{CI_{t=24}}{CI_{Control}} \qquad (3)$$

$CI_{t=48}$ = Cell index of exposed cells at timepoint t=48.

$CI_{control}$ = Cell index of control group at timepoint t=24.

3.1.7 Miniaturisation of the *D. magna* Immobilization assay for ENMs

The survivorship of 5 *D. magna* neonates (1 day old at start) in 250 mL of high hardness (HH) Combo medium was compared to that of isolated *D. magna* neonates each individually cultured in 50 mL of HH Combo medium and to isolated D. magna individually cultured in 50 mL of conditioned HH Combo medium that came from a 1L running culture that had previously contained 20 *D. magna* (15–20 days old), by monitoring survivorship for 120 days (n = 25 daphnids for each condition (five jars with 5 *D. magna* each in the case of grouped neonates).

For acute toxicity testing, 20 neonates were used per replicate of each chemical concentration, and the exposure conducted for 48 h in OECD media in the absence of food, using multiple different exposure vessels. The reference condition was set to 200 ml volume of medium in a glass beaker, and was compared with all other volumes and exposure vessels (glass beaker, 6, 12, 24 and 48 well multiwell plates and Petri dishes), with and without conditioning of the medium. Initially we focused on CuO ENMs

This project has received funding from the European Union's Horizon 2020 research and innovation programme under grant agreement No 814425.

to study the impacts of total volume (V), surface to volume ratio (S:V) and animal density on the acute toxicity of *D. magna* neonates in different types of exposure vessels (glass jars and various well plates (6, 12, 24 and 48 multiwell plates). Having measured the acute toxicity under the reference conditions and calculated several effective concentration (EC) values, we selected three test concentrations that correspond to three levels of toxicity under the reference conditions (EC25, EC50, EC75) to assess the effects of differing test configurations. Subsequently, we used our recommended miniaturised test setups to study the single animal toxicity of the panel of RiskGONE ENMs.

For algae feeding, we investigated the test configurations using daphniids from neonates to adults. The test was performed in various well plates (6, 12, 24 and 48 multiwell plates) to determine the impacts of total volume, algae concentration and adult *Daphnia* density. Daphniids were incubated for 1 h in HH Combo medium and the feeding of algae (*Chlorella vulgaris*) was measured using a cell counter (CASY, Roche). The CASY counter requires 0.2 mL from the media appropriately diluted in the linear measuring range of the instrument. In addition, the feeding rate was assessed as a function of animal age (1, 2, 3, 5, 7, 10, 14, 21 and 28 days), and also after exposing daphniids of different ages to selected RiskGONE ENMs to estimate the impact of stress on their feeding performance.

3.2 Impedance-based flow cytometry

The Ampha Z30 (Amphasys AG, Lucerne, Switzerland) was used, which is an impedance flow cytometer for single-cell characterization without optical components that assess cellular size, membrane capacitance, and cytoplasm resistance (UiB) (Ostermann et al. 2020). The ENMs which showed the highest cytotoxicity according to the xCELLigence data were ZnO, CuO and MWCNT. Therefore, these ENMs were picked to be tested for toxicity by impedance-based flow cytometry. The MWCNT could not be used with the AmphaZ 30 because they caused frequent clogging of the analysis chip, which did not allow the cells to pass through. Thus, the tests were run with ZnO and CuO. The cells were exposed to the ENMs at five different concentrations (2, 10, 20, 50, 100 µg/mL).

The intention was to compare the effects on fish cells with those on human cells, however, hindrances due to the Covid 19 pandemic and loss of cells due to a malfunction in the storage system have delayed the testing on fish cells. Therefore, only the results obtained on U937 human monoblastoid cells are presented in this deliverable.

3.2.1 Cell culture and testing

The U937-cells were seeded at a cell density of 100.000 cells/mL in a 6-well plate in 2 mL of complete DMEM medium (with 10% FBS and 1% PS) and kept in an incubator at 37°C and 5% CO_2 for 24 h. After 24 h, the 6-well plate was centrifuged at 250 g for 5 min. Optical microscopy was used to ensure that the cells did not float. From each well, 1 mL of supernatant medium was carefully removed, then 1 mL of ENM dispersions were added and final concentrations of 1, 2, 5, 10, 25 and 50 µg/cm² (corresponding to 2, 10, 20, 50, and 100 µg/mL) were obtained. The plate was then incubated for an additional 24 h period.

Prior to cell collection, the AmphaZ30 device was rinsed and cleaned using Ampha Clean (Amphasys AG, Lucerne, Switzerland) and EtOH. The 6 well plate was centrifuged at 250 x g for 5 min and then the supernatant was removed and replaced by 1 mL of PBS in each well. Cells were resuspended and pipetted into centrifuge tubes. The tubes with cells and PBS were centrifuged at 250 x g for 5 min after which the supernatant was removed and replaced with 100 µL of PBS. In each tube, 400 µL of sucrose

This project has received funding from the European Union's Horizon 2020 research and innovation programme under grant agreement No 814425.

buffer were added to ensure a 1:4 PBS/sucrose ratio. A 20 x 20 µm channel chip was employed in measurements. To avoid clogging, the chip was rinsed with MilliQ water on a regular basis.

Cells heated at 70 °C for 30 min served as positive control for necrosis. To test for possible ENM interferences, the highest ENM concentration (100 µg/mL) was added to cell-free medium, as well as to negative and positive cell controls. The impedance-based measurements (Ampha Z30, Amphasys AG, Switzerland) were carried out using 0.5, 2, 6, and 12 MHz. The ENMs and cell debris were excluded at the chosen settings, the trigger level of 0.02 V excluded any noise by a good margin. Additional curve detection further excludes random noise as noise does not follow the same time-dependent pattern as cells do.

A total of 10.000–20.000 cells per sample were analysed using the AmphaSoft 2.0 (Amphasys AG, Switzerland). The 6 MHz-frequency was found to be optimal for assessing plasma membrane permeability. A gate for viable cells (intact cell membrane) was created in AmphaSoft 2.0 using the negative control and then applied to all samples within one exposure experiment. The viable cells within the gate were presented as a percentage of the total number of cells, which was used for further analysis.

3.3 Impedance-based microfluidic system

The impedance-based xCELLigence measurements under static exposure conditions showed that the cells that were mostly affected by the ENMs, were the ZF4-cells. Therefore, we wanted to investigate the impact of the most toxic ENMs on these cells under dynamic exposure that resemble *in vivo* conditions. For this, a microfluidic system designed and constructed at UiB chip was fabricated to mimic the *in vivo* dynamic environment (Ruzycka et al. 2019). A microfluidic chip consisting of four independent channels with electrodes was designed and fabricated (Figure 8). The ENM dispersion in cell culture medium was introduced into these channels through the inlets and then flowed through the area containing the sensing electrodes and came out of through the outlet. The flow of liquid was driven by a peristaltic pumping system (peRISYS-S, Cetoni, Korbussen, Germany). This system circulates the fluid from and to the reservoirs placed outside of, and connected to, the microfluidic chip.

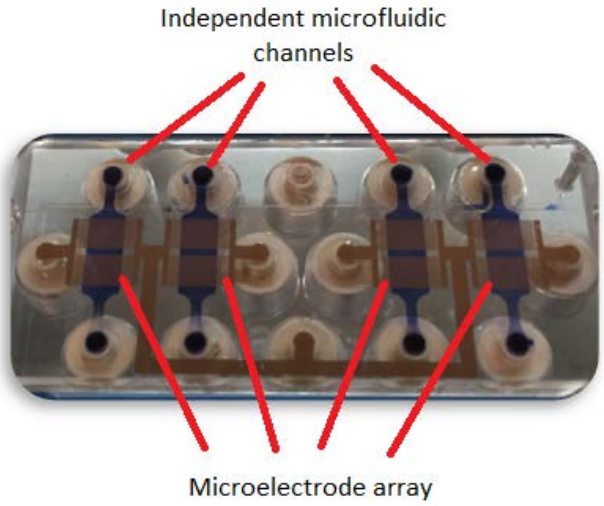

Fig. 8. Microfluidic chip with four independent channels with inlets on one side and outlets on the other. Golden-plated electrode is shown on top of each channel with the inlet for the electrode connector (UiB).

This project has received funding from the European Union's Horizon 2020 research and innovation programme under grant agreement No 814425.

3.3.1 Fabrication of the microfluidic chip

The fabrication of the microfluidic chip was performed in three steps as shown in Figure 9:

1) Photolithography on silicone substrate to create a hard mold (SI-master) containing the microfluidic network.

2) Soft lithography to make the microfluidic chamber by replicating the features in the hard mold onto the elastomeric polymer polydimethylsiloxane (PDMS).

3) Photolithography and e-beam vapor deposition to create a microelectrode array onto a glass coverslip (performed at the NanoPhysics Section at the Department of Physics and Technology, UiB). Finally, the microfluidic channels were created by fusing the PDMS cast onto the glass coverslip containing the microelectrode array using oxygen plasma.

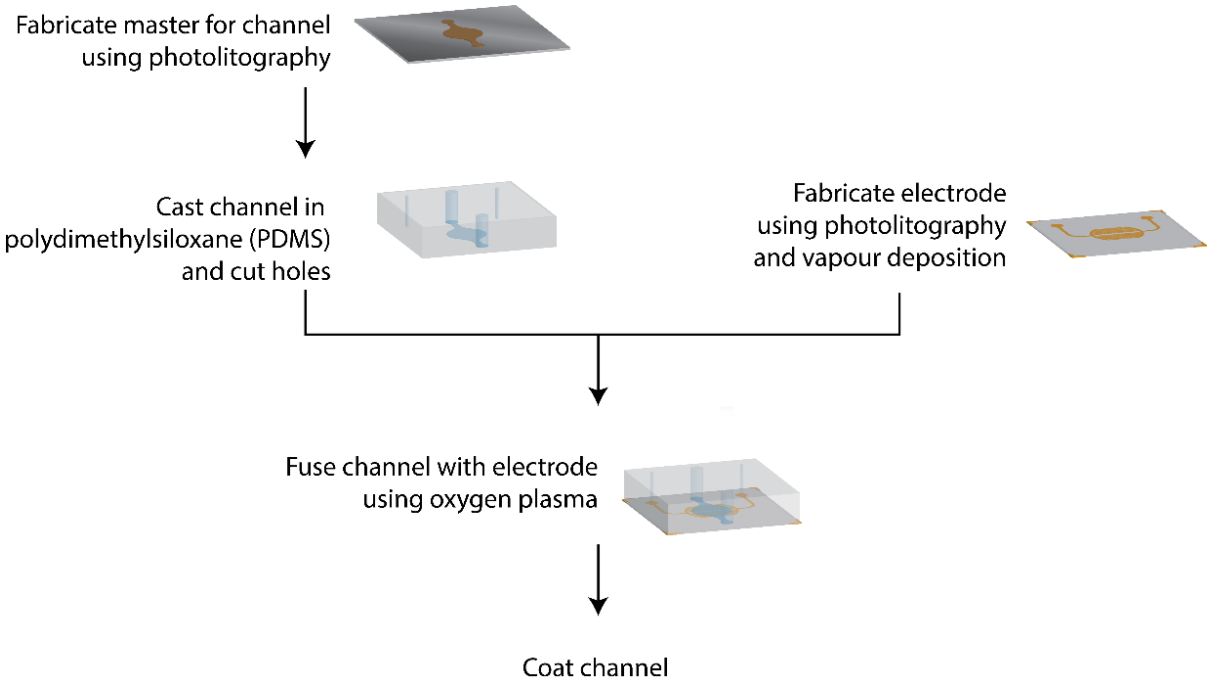

Fig. 9. Fabrication steps of the microfluidic chip. The fabrication of the hard mold (master) for channels using photolithography, PDMS cast, fabrication of electrode and the fusing of PDMS cast with the electrode on a glass coverslip using oxygen plasma.

For the fabrication of the microfluidic chip, a hard mold with the pattern for the microfluidic channels were needed (Figure 10). The mold was made by photolithography with a negative photoresist. The method utilizes UV-light to transfer the pattern from an optical mask (photomask) to the photosensitive resist in the substrate. The microfluidic and microelectrode layouts were generated using Layout Editor (Juspector Gmbh, Germany) and the Cr-photomask was fabricated by JD Photomask (Herts, UK). A 125 mm silica wafer (Sumco Corporation, Tokyo, Japan) was washed with piranha solution (3:7 H_2O_2:H_2SO_4) for 1 h, rinsed with MilliQ water and cleaned with acetone and dried with N_2 gas. The negative photoresist SU-8 2100 (MicroChem Corporation, MA, USA) was deposited on the wafer with a thickness of 100 µm. This was achieved by pouring about 5 mL of SU-8 2100 on the wafer and spin-coating it for 10 sec at 500 rpm, then 45 sec at 3000 rpm. The wafer was then baked on a hot plate (PZ 28-2 ET, Harry Gestigkeit GMBH, Düsseldorf, Germany) at 65°C for 5 min then 95°C for 20 min. The UV-exposure of the coated

This project has received funding from the European Union's Horizon 2020 research and innovation programme under grant agreement No 814425.

wafer was performed using a MJB4 mask aligner (SUSS Microtec, Garching, Germany) and filter (PL-360, Omega Optical Inc., VT, USA) with an exposure energy of 240 mJ/cm^2. After UV-exposure the wafer was baked on the hot plate at 60°C for 5 min then 75°C for 50 min. Unexposed resist was stripped away using SU-8 2100 developer (MicroChem Corporation, Ma, USA) in a water bath sonicator for 5-10 min. Lastly, the wafer was rinsed with isopropanol and MilliQ water and dried using N_2 gas.

The microfluidic channels of the chip were casted using soft lithography with PDMS. The PDMS was made by mixing silicon elastomer base with elastomer curing agent (Dow corning, Sylgard 184) in a 10:1 ratio. The mixture was placed in an exicator connected to a vacuum pump to release the bubbles trapped in the PDMS. The hard mold containing the print of the microvascular channels was placed in a casting system made with Teflon and a polycarbonate lid on top. The polycarbonate lid had been treated with O_2 plasma using a low-pressure plasma system (Diener Electronics GMBH & Co. KG, Ebhausen, Germany) for 1 min (0.3 bar, 60 W) before mounted to the casting system. Channel spacers were attached to the polycarbonate lid to leave holes in the inlet and outlet of the channels. The degassed PDMS was then injected into the casting system via the polycarbonate lid and cured at 65°C for 6h. After the 6h the channel spacers were removed, and the PDMS was left connected with the polycarbonate lid exposing the microvascular channels. Excess PDMS was removed, and holes used for electrical and fluidic connectors were cut.

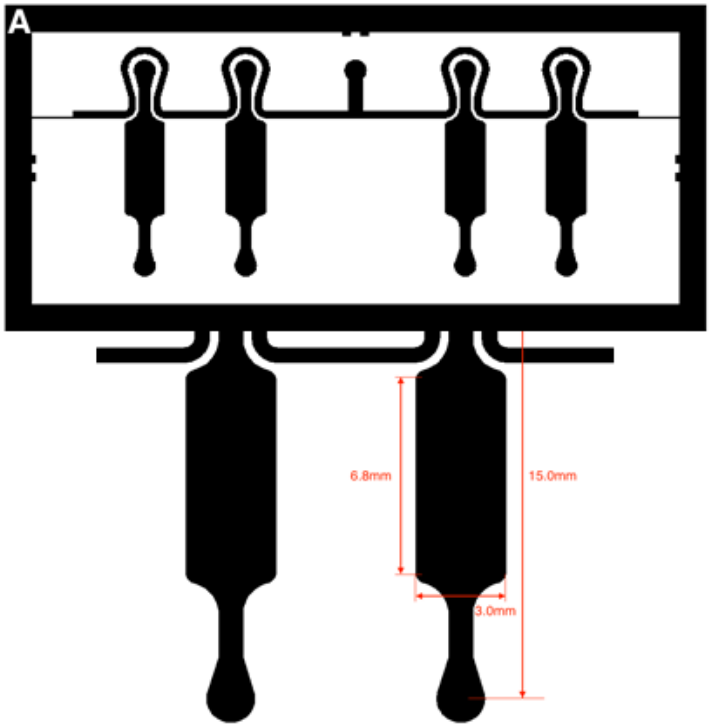

Fig. 10 Hard mold design used for the microfluidic chip. A) the four independent microvascular channels. B) close-up of the channels previewing the sizes of the dimensions. The height of the channels was 100 µm. The hard mold was used for PDMS soft lithography.

The PDMS with the microfluidic pattern was then fused with the glass coverslip containing Au electrodes. Both the PDMS and the glass coverslip (50x20mm Decker glass) were cleaned with isopropanol and dried with N_2 gas. The surface of the PDMS and the glass coverslip were treated with O_2 plasma (1 min,

This project has received funding from the European Union's Horizon 2020 research and innovation programme under grant agreement No 814425.

0.3 bar, 60 W). The surfaces that were treated were then put together, fusing the glass coverslip containing the electrode with the PDMS.

3.3.2 Setup of the microfluidic system

The microfluidic system consisted of a microscope equipped with a DSD2 unit and a Zyla 5,5 sCMOS camera, enclosed in an environmental chamber to maintain the temperature at 28°C (see Figure 11).

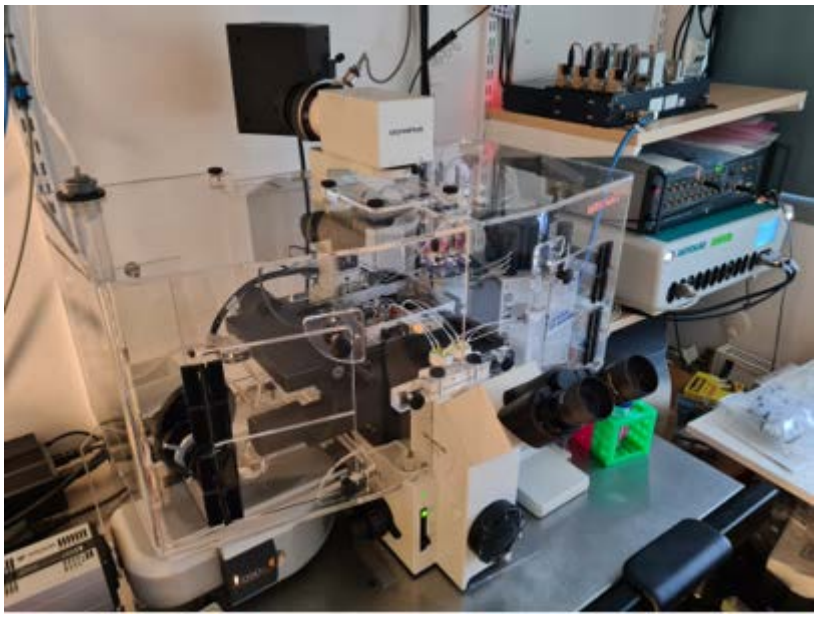

Fig. 11. Microfluidic setup consisting of a microscope, DSD2 unit and camera enclosed in an environmental chamber. Inside the chamber there is a microscope-stage for the microfluidic chip, the tubing-system containing reservoirs and CO_2-tubes and the peristaltic pump.

3.3.3 Microfluidic channel coating and cell seeding

To monitor the ZF4-cells inside the microfluidic chip, it was essential to determine how to seed the cells. The channels in the microfluidic chip were coated with Poly-L-Lysine (PLL, 0.02% w/v) and left in a refrigerator for 24 h. The PLL was removed from the channels and washed with warm PBS thoroughly. Then the channels were coated with Laminin (50 µg/mL in PBS), 50 µL in each channel and left for 1h at room temperature.

Prior to seeding, the tubing system and fluidic connectors were established by cutting peristaltic tubes and using syringes for the reservoir. The tubing system and fluidic connectors were cleaned by ethanol and autoclaved. After the microfluidic chip was coated with PLL and Laminin, warm PBS was injected into the channels and the chip was connected to the potentiostat through the electrode connectors. This was to determine the nominal impedance of each microelectrode array in PBS (20 mV at 10, 15 and 25 kHz). The microfluidic chip was then moved to a laminar hood and seeded with the ZF4 cells. The PBS was removed, and the channels were injected with FBS-free DMEM/F12. 8 µL of ZF4 cell suspension (2 x 10^6) was pipetted into each inlet of each channel. Immediately after injection, 5 µL were removed from

This project has received funding from the European Union's Horizon 2020 research and innovation programme under grant agreement No 814425.

the outlets of each channel gently to drive the suspension into the microchannels. The microfluidic chip was then incubated for 10 min for the cells to attach to the channels. When the cells attached, new fresh DMEM/F12 (10% FBS) was introduced, and the chip was incubated for 1h. Afterwards, medium was replaced by FBS-free DMEM/F12 to connect the chip to the tubing system in the microfluidic setup. The tubing system and fluidic connectors were filled with FBS-free DMEM/F12 prior to connecting the chip to avoid bubbles in the microfluidic channels. Finally, the medium was exchanged with DMEM/F12 containing 10% FBS and the cells were monitored for 24 h.

For this setup, the cells were monitored by impedance measurements at every 15 min for 24 h. The voltage was set to 20 mV, and the impedance was recorded at 10, 15 and 25 kHz. Electrode connectors were plugged to a potentiostat (Autolab PGSTAT128N, Metrohm, Herisau, Switzerland) through a microelectrode switch (MUX16 module). The computer software Nova (version 2.1.1) was used to control the impedance measurements in the chip. The fluid was re-circulated by a peristaltic pumping system, the peristaltic pump circulated fluid from the reservoirs into the inlet, through the channels and back into the reservoirs. The computer software (QmixElements, Cetoni, Korbussen, Germany) was used to control the pump. For the microscope and continuous pictures taken, the software Andor iQ (version 3.2, Andor, Oxford Instrument, Abingdon, UK) was used.

3.3.4 Bubble trap fabrication

A bubble trap was fabricated to prevent air bubbles being dragged inside the microfluidc chip, which dislodge and damage the cells. Two discs (3.3 cm diameter by 6 mm thickness) of polyvinyl chloride (PVC) were CNC-machined using a compact CNC machine (Wegstr, Czech Republic) based on a layout designed on Cut2D software (Vectric, UK). One of the PVC discs contained a long serpentine microfluidic network (0.2 x 0.2 x 15 mm) and the other disc five vent channels (1 x 2 x 15 mm). Both discs were interfaced by a micro-porous, hydrophobic PTFE membrane (Darwin Microfluidics, France) and fastened together. This trap works by allowing excess gas trapped in the cell culture medium flowing through the serpentine channel to pass through the micro-porous PTFE membrane towards the opposing disc with air vents opened to the atmosphere.

3.4 Modeling of ENM-induced toxicity in cells based on xCELLigence system measurements

A mathematical model was developed by HVL that takes into consideration the speed of the FC change. The calculation was performed in Matlab by integrating the derivative of the FC vs control over the entire exposure period to ENMs.

3.5 Statistical analysis

The statistical software package IBM SPSS (Version 26, Chicago, IL, USA) was used to evaluate the data from the xCELLigence and Amphasys experiments. One-way ANOVA (Post Hoc Tukey) was used for a multiple comparison of samples, to determine the significance of each concentration($p \leq 0.05$).

This project has received funding from the European Union's Horizon 2020 research and innovation programme under grant agreement No 814425.

4. Results

4.1 Physicochemical characteristics of nanomaterials

The HDD, PDI and ZP of the ENM dispersions in the different cell culture media were measured using the DLS technique for the highest exposure concentration (100 µg/mL), shortly after preparation at 0 h and 24 h after, which corresponds to the end of ENM exposure duration in experiments with cells. The results are listed in Table 3.

Table 3: Physicochemical properties of ENMs in Stock (milliQ) and complete cell culture medium DMEM, DMEM/F12 and L-15.

	DLS				**ELS**	
Samples	Mean hydrodynamic diameter ± SD [nm]		PDI ± SD		Zeta potential ± SD [mV]	
	0h	**24h**	**0h**	**24h**	**0h**	**24h**
CuO						
DMEM	765,4 ± 51,9	112,1 ± 38,5	0,881 ± 0,030	0,291 ± 0,083	-8,5 ± 0,4	-9,5 ± 0,8
DMEM/F12	731,3 ± 50,7	636,4 ± 265,6	0,890 ± 0,028	0,669 ± 0,241	-8,3 ± 0,7	-7,0 ± 0,9
L-15	380,1 ± 163,3	15,8 ± 0,200	0,382 ± 0,115	0,394 ± 0,003	-8,1 ± 0,5	-8,2 ± 1,2
STOCK (milliQ)	2764	25630	1	0,581	-	-
MWCNT						
DMEM	2280 ± 337,9	3342 ± 454,9	0,353 ± 0,153	0,328 ± 0,032	-11,3 ± 0,7	-11,5 ± 0,7
DMEM/F12	3150 ± 403,4	3738 ± 181,5	1,000 ± 0,000	0,596 ± 0,133	-12,7 ± 0,7	-12,7 ± 0,5
L-15	3271 ± 277	3402 ± 291	0,484 ± 0,142	0,598 ± 0,115	-14,0 ± 0,6	-14,1 ±0,6
STOCK (milliQ)	293,2	271,3	0,354	0,276	-	-
WC/co						
DMEM	341,3 ± 17,9	622 ± 405,6	0,502 ± 0,019	0,666 ± 0,173	-9,9 ± 0,9	-11,2 ± 0,5
DMEM/F12	539,2 ± 61,88	787,8 ± 295,8	0,792 ± 0,022	0,807 ± 0,096	-9,9 ± 0,6	-9,9 ± 0,4
L-15	407,3 ± 54,83	184,2 ± 35,71	0,457 ± 0,022	0,876 ± 0,115	-11,2 ± 0,8	-9,4 ± 0,6
STOCK (milliQ)	667,5	429,2	0,693	0,377	-	-

DLS = Dynamic light scattering, ELS = Electrophoretic light scattering

4.2 Impedance-based measurements using the xCELLigence system

The *CI* gives an indication of the proliferation, viability and the adhesion of the cells to the electrodes.

4.2.1 RTgut-cells exposed to ENMs

Figure 12 shows the NCI for RTgut cells exposed to CuO, WC-co, MWCNT and the MWCNT dispersant. It represents the real-time proliferation of cells exposed to the ENMs making it possible to determine when and at which concentration(s) the ENMs impact the cells proliferation.

The NCI of RTgut cells exposed to CuO is displayed in Figure 12a. During the initial 3h of exposure, there was a faster increase of NCI of the cells exposed to 20, 50 and 100 µg/mL CuO when compared to control. Afterwards, the NCI rate slowed down, but was still higher than control for the next 7 h. This proliferation continued in the case of cells exposed to 20 µg/mL, but not for those exposed to 50 and

This project has received funding from the European Union's Horizon 2020 research and innovation programme under grant agreement No 814425.

100 µg/mL, where the NCI decreased to levels lower than control. The NCI of the cells exposed to 2 and 10 µg/mL CuO increased at a similar rate to that of control.

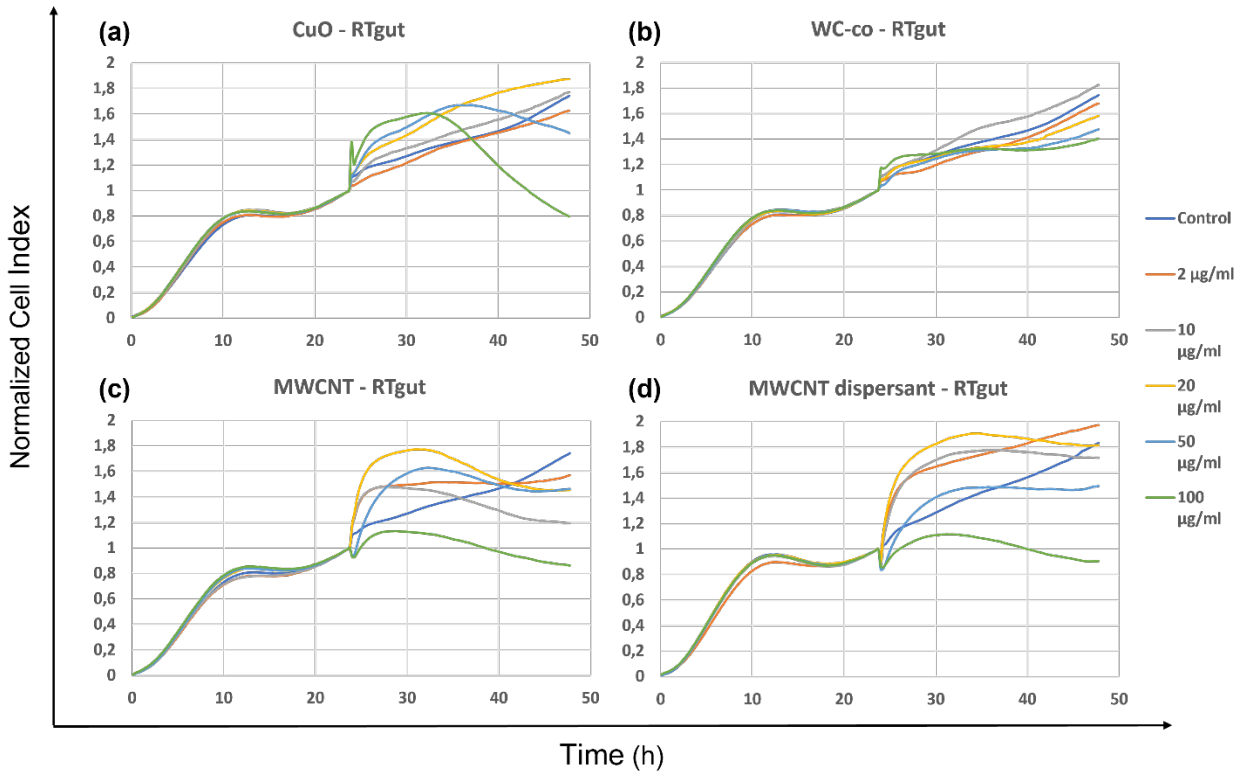

Fig. 12. Normalized Cell Index (NCI) of RTgut-cells grown in L15 medium in xCelligence E-plates exposed to three ENMs: (a) CuO, (b) WC-co, (c) MWCNT and (d) MWCNT-dispersant. Cells were seeded at 10 000 cells/well (50 000 cells/cm^2) and after 24 h were exposed to 5 different concentrations of ENMs. In (d) the MWCNT-dispersant is without ENM and the concentrations are the corresponding amount of dispersant used in the 5 concentrations of MWCNT. Each experiment was run in triplicates and repeated three times. The plots show the mean of three individual experimental repetitions.

The data of RTgut cells exposed to WC-co is presented in Figure 12b. As for CuO, there is an initial growth of NCI of the cells exposed to 100 µg/mL. However, this growth stagnated after 2 h, unlike the control. The cells exposed to the 20 and 50 µg/mL WC-co proliferated at rates comparable to control during the first 8 h of exposure, but then slowed down. The cells exposed to 10 µg/mL showed a proliferation above the control, while the cells exposed to 2 µg/mL showed a similar growth as the control.

Figures 12c and 12d show the growth of cells exposed to MWCNT with dispersant and the dispersant alone, respectively. To note, the amount of dispersant used in Figure 12d corresponded to the volume contained in the MWCNT dispersion for each concentration tested. Cells exposed to 100 µg/mL MWCNT showed a slight drop of NCI, followed by short recovery and subsequent gradual drop of NCI. This same trend was observed when testing the dispersant alone. Thus, the toxic effect can be largely attributed to the dispersant. Cells exposed to lower concentrations of MWCNT showed an initial sharp increase of

This project has received funding from the European Union's Horizon 2020 research and innovation programme under grant agreement No 814425.

NCI, which plateaued for a few hours and then gradually decreased, except for the lowest concentration tested. A similar behavior was observed for cells treated with the dispersant alone. However, the decrease of NCI after the plateau was not as steep and stagnation for the lowest ENM concentration did not occur.

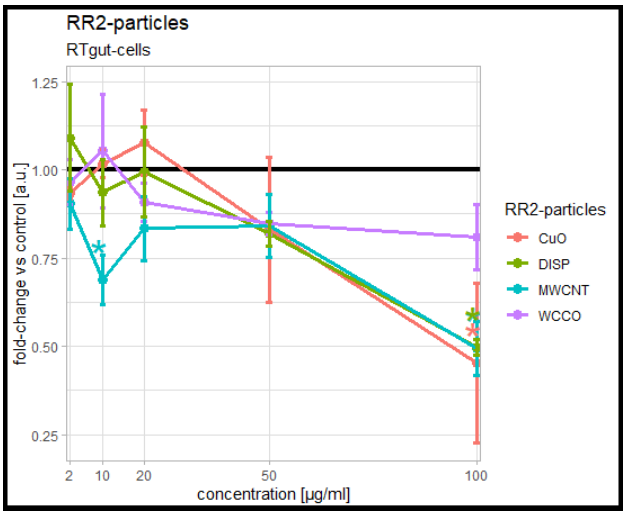

Fig. 13. The fold change (FC) of the impedance measurements for RTgut-cells exposed to ENMs: CuO (red), WC-Co (purple), MWCNT (blue), and the dispersant for MWCNT (green) 24 h after exposure. Complete L-15 medium (10% FBS) was used for the cells. Cells were exposed to 2, 10, 20, 50 and 100 ug/mL concentrations. The figure shows the mean of three independent repetitions. The control is marked as the black line at FC = 1. "*" marked statistical significance in respect to control, $p < 0.05$ (One-way ANOVA).

The comparison of ENMs' toxicity on RTgut cells is presented in Figure 13. For CuO, the RTgut cells exposed to 50 and 100 µg/mL show a lower FC compared with the control, which is statistically significant difference at the highest concentration 100 µg/mL. The WC-co lowers the proliferation at 50 and 100 µg/mL, however, this is not statistically significant. For MWCNT, a significantly lower proliferation is seen at has statistical significance at 10 µg/mL and 100 µg/mL. The MWCNT dispersant significantly impacted the proliferation at the highest concentration of 100 µg/mL, which indicates that the effect seen for effect seen at 10 µg/mL for MWCNT was caused by the particles and not the dispersant.

4.2.2 ZF4-cells exposed to ENMs

Figure 14 shows the NCI for ZF4-cells exposed to CuO, WC-Co, MWCNT and MWCNT dispersant. The figures display the real-time proliferation or decrease of the NCI for each ENM. Due to the real-time aspect, it is possible to determine when the NCI increases or decreases for each ENM and concentration.

This project has received funding from the European Union's Horizon 2020 research and innovation programme under grant agreement No 814425.

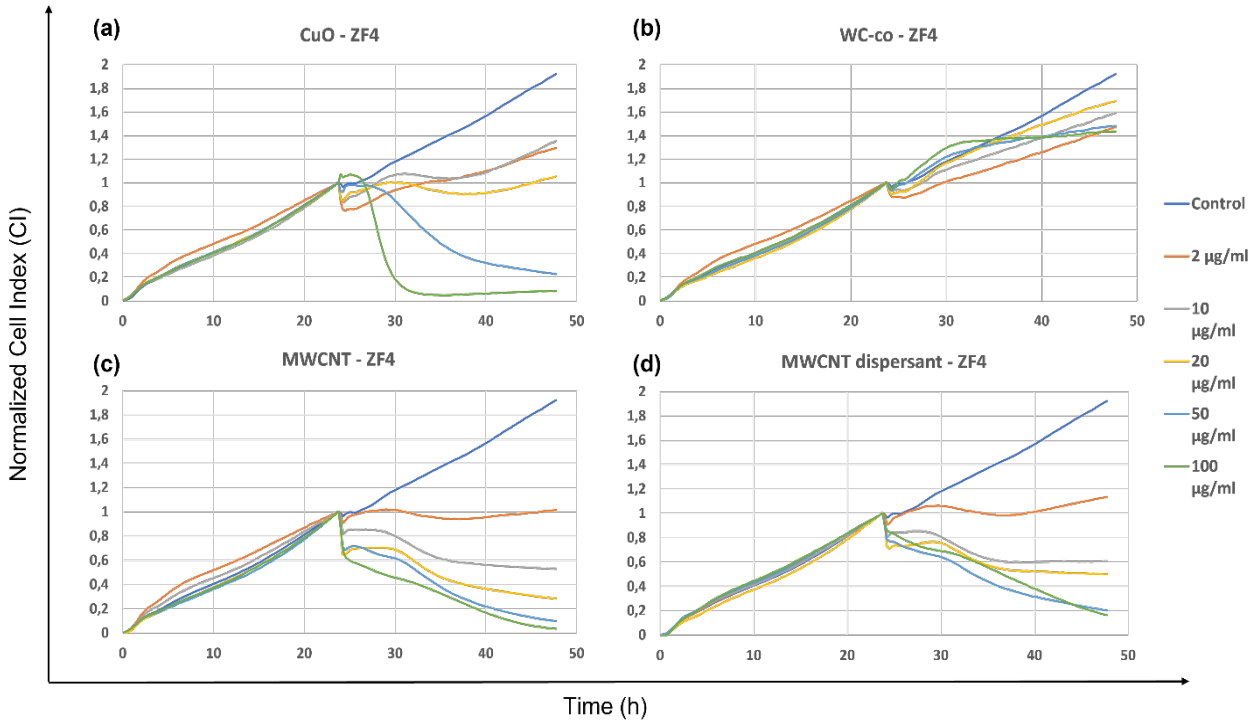

Fig. 14. The NCI of ZF4-cells grown in DMEM/F12 medium in xCelligence E-plate exposed to ENMs: (a) CuO, (b) WC-co, (c) MWCNT and (d) MWCNT-dispersant. Cells were seeded at 10 000 cells/well (50 000 cells/cm^2) and after 24 h were exposed to 5 different concentrations of ENMs. (d) MWCNT-dispersant is without ENM and the concentrations represent the corresponding amount of dispersant used in the 5 concentrations of MWCNT. Each experiment was run in triplicates with three individual experimental repetitions. The plots represent the mean of three individual experimental repetitions.

The data in Figure 14a displaying the NCI of ZF4 cells exposed to CuO show a clear difference between the cells exposed to ENMs and the control. The NCI of ZF4 cells exposed to WC-co is close to the control. The proliferation of cells exposed to MWCNT with dispersant and the dispersant alone, show similar effects, both types of exposure inducing an initial decrease of NCI for 10, 20, 50 and 100 µg/mL. Since the effects from the exposure to MWCNT or the dispersant alone are so similar, the toxic effect can be largely attributed to the dispersant.

This project has received funding from the European Union's Horizon 2020 research and innovation programme under grant agreement No 814425.

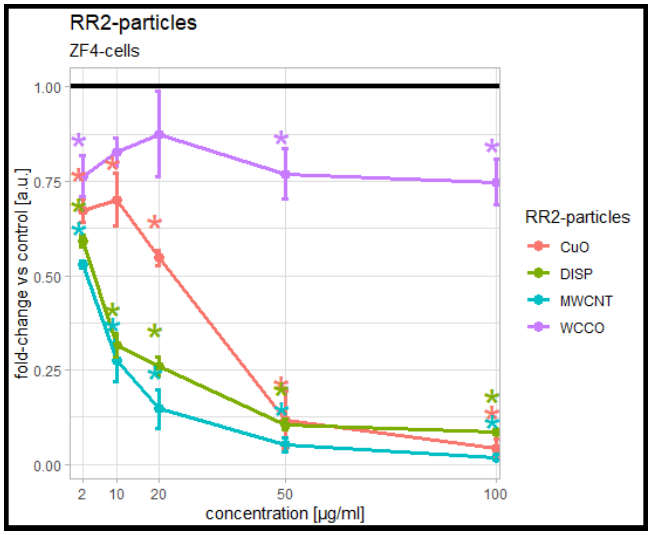

Fig. 15. The fold change (FC) between impedance measurements of unexposed ZF4-cells (controls) and of ZF4-cells exposed to ENMs at 2, 10, 20, 50 and 100 µg/mL: CuO (red), WC-co (purple), MWCNT (blue) and the dispersant from MWCNT (green) at 24 h after exposure. Complete DMEM/F12 medium (10%) was used for the cells. The mean three independent repetitions is shown. The control is the black line at FC = 1. "*" marked statistical significance in respect to control, $p < 0.05$ (One-way Anova).

The comparison of ENMs' toxicity on ZF4 cells is presented in Figure 15. The ZF4 cells were significantly affected by the three ENMs at most of the concentrations. For CuO a statistically significance reduction of proliferation was seen at all concentrations. The lowest FC value was seen at the highest concentrations of 50 and 100 µg/mL for both CuO and MWCNT. MWCNT and the MWCNT dispersant had similar trends and close FC values, with MWCNT having slightly lower FC values than the dispersant, which indicates that the dispersant contributed significantly to the toxic effect.

4.2.3 Comparison of cell lines' responses to ENMs

One of the aims in RiskGONE was to evaluate and compare the effects of the selected ENMs on human cells and biological models (WP5) with those detected in fish cells and aquatic organisms (WP6). We have therefore compared the results obtained with the xCELLigence system for RTgut and Z4F cells with those obtained in WP5 on A549 human lung epithelial cells. Figure 16 displays the FC of each cell type at the end of exposure to each ENM and shows the difference in effect between each cell type. For the CuO exposure, ZF4 is clearly the cell-type with the lowest FC values, which are statistically significant at every concentration. The FC levels in A549 cells exposed to CuO are also low, with all but the lowest concentration being statistically significant. The RTgut cells appear to be the least affected by CuO, with only the highest concentration significantly reducing the proliferation. After exposure to WC-Co, ZF4 cells had the lowest FC values, statistically significant at most concentrations. The A549 cells had the highest FC values and as RTgut cells and statistically significant difference was seen only at the highest concentration. The ZF4 cells had the lowest FC values, statistically significant at all concentrations, following exposure to MWCNTs. The A549 and RTgut cell types had similar FC values, with a clear statistical significance at the highest concentration.

This project has received funding from the European Union's Horizon 2020 research and innovation programme under grant agreement No 814425.

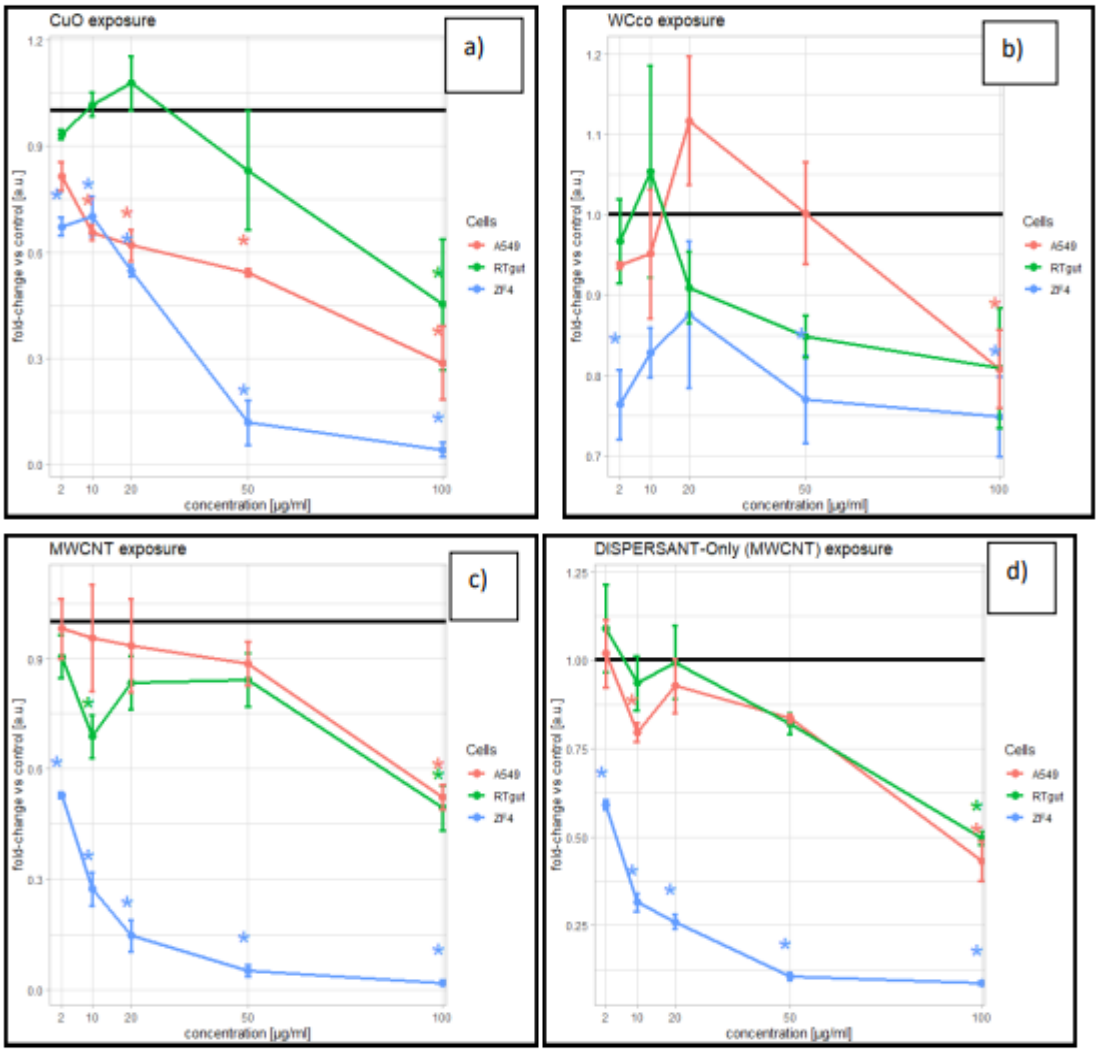

Fig. 16. Comparison of ENM effects on three cell lines – 2 fish cell lines and A549 human lung epithelial cells (from RiskGNE WP5). ENMs: CuO (a), WC-co (b), MWCNT (c), and MWCNT-dispersant (d). The A549 (red), RTgut (green) and ZF4 (blue) cells were exposed for 24h to 5 ENM concentrations: 2, 10, 20, 50 and 100 µg/mL. The mean of three independent repetitions is shown. Control is marked as the black line = 1. "*" marks the statistical significance in respect to the control, $p < 0.05$ (One-way Anova).

4.3 Impedance-based flow cytometry testing

The ENMs that showed the highest cytotoxicity according to the xCELLigence data were ZnO, CuO and MWCNT. Therefore, these ENMs were selected for impedance-based flow cytometry toxicity testing. The MWCNT could not be used with the AmphaZ 30 because they caused frequent clogging of the analysis chip, which did not allow the cells to pass through. Therefore, the tests were run with ZnO and CuO. The cells were exposed to the ENMs at five different concentrations (2, 10, 20, 50, 100 µg/mL). The intention was to compare the effects on fish cells with those on human cells, however, hindrances due to the Covid 19 pandemic and loss of cells due to a malfunction in the storage system have delayed the testing on fish cells. Therefore, only the results obtained on U937 human monoblastoid cells are given here.

This project has received funding from the European Union's Horizon 2020 research and innovation programme under grant agreement No 814425.

4.3.1 U937-cells exposed to CuO

Figure 17 displays a dot-plot of impedance flow cytometry measurements of U937-cells exposed to CuO ENM at 10, 50, and 100 µg/mL. The figure also shows the negative and positive controls. The dot-plot is gated with reference to the negative control to determine whether the cells are alive or not. All the cells to the right of the gating (black vertical line) are alive, while the cells on the left of the gating are either dead or in the process of dying. It is possible to see a shift to the left (dead cells) in the population of cells exposed to CuO compared to the control. For the cells exposed to 10 and 50 µg/mL there is a small shift towards the left side of the gating, while the cells exposed to the 100 µg/mL have a bigger shift, which overlaps with the population of dead cells from the positive control.

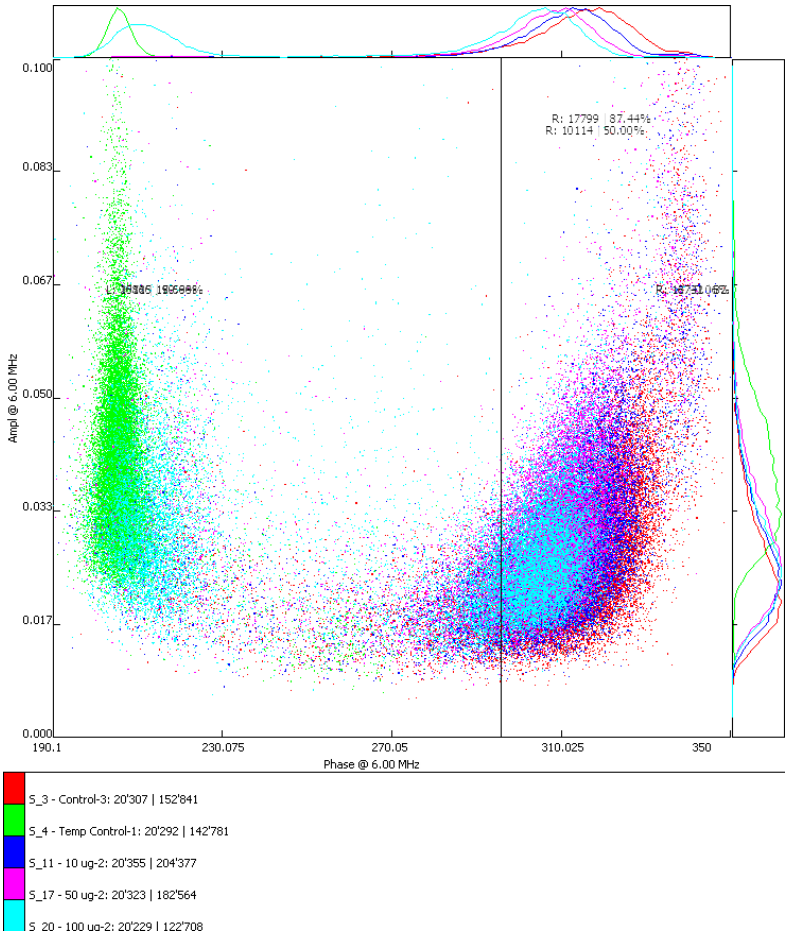

Fig. 17. Dot-plot of U937-cells exposed to CuO at 6.00 MHz. Amplitude [V] vs phase [°]. Each dot represents a U937 cell. Red = Negative control, Green = Positive control, blue = 10 µg/ml, purple = 50 µg/ml, teal = 100 µg/ml.

The results are summarized in Figure 18, which shows the percentage of cells alive at the end of exposure to different concentrations of CuO. The viability of cells exposed to 2, 10, 20 and 50 µg/mL was >70%. The cells exposed to 100 µg/mL had a viability of 23.3%, which is statistically significant lower compared to the control.

This project has received funding from the European Union's Horizon 2020 research and innovation programme under grant agreement No 814425.

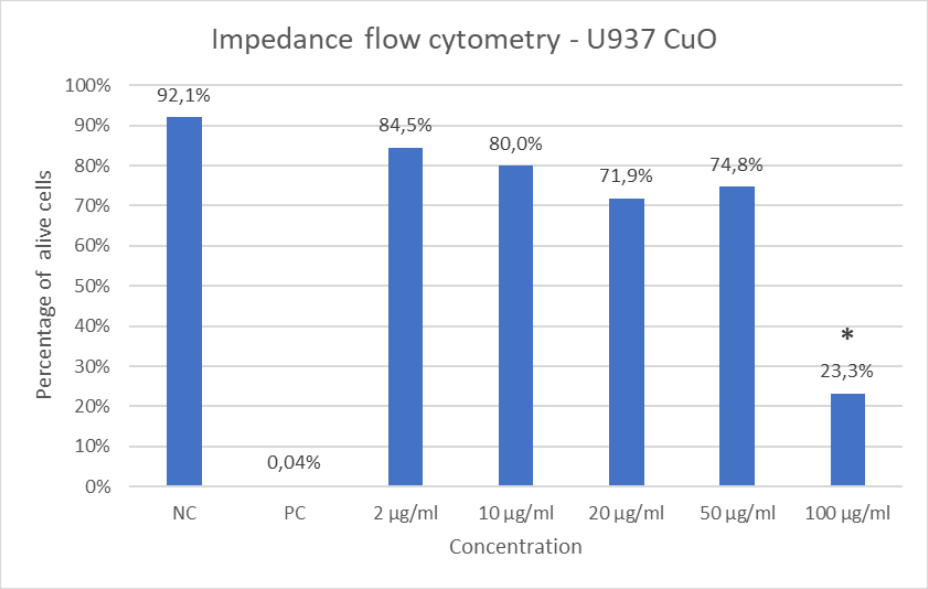

Fig. 18. Percentage (%) of viable cells following exposure for 24 h to CuO ENM at different concentrations (2, 10, 20, 50 and 100 µg/mL). NC = negative control, PC = Positive control. Complete DMEM (10% FBS) was used for the cells. Cells were seeded at 100 000 cells/mL. "*" marked statistical significance compared to the control, $p < 0.05$ (One-way Anova).

4.3.2 U937-cells exposed to ZnO ENM

In Figure 19 a dot-plot is presented to display the amplitude and phase shift for U937 cells exposed to ZnO ENM for 24 h. It shows the negative control, positive control and the cells exposed to ZnO at concentrations 10, 50 and 100 µg/mL. The dot-plot is gated in reference to the negative control. A population shift is noted to the left for cells exposed to 10, 50 and 100 µg/mL compared to the negative control. This shift is particularly large at the highest exposure concentration indicating a high number of dead cells.

This project has received funding from the European Union's Horizon 2020 research and innovation programme under grant agreement No 814425.

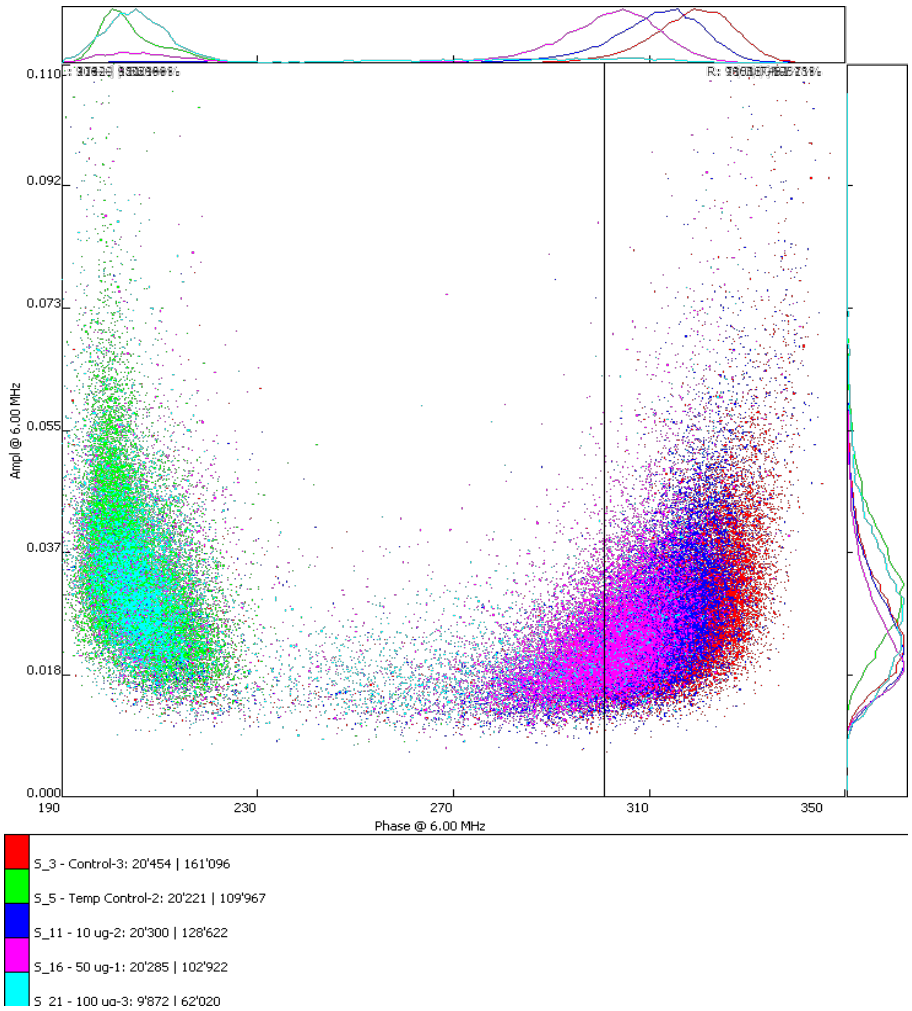

Fig. 19*. Dot-plot of U937-cells exposed to ZnO at 6.00 MHz. Amplitude [V] vs phase [°].* Each dot represents a U937 cell. Red = Negative control, Green = Positive control, blue = 10 µg/ml, purple = 50 µg/ml, teal = 100 µg/ml.

The results are summarized in Figure 20, which displays the percentage of cells that are alive after exposure to different concentrations of ZnO, as well as negative and positive controls. The viability percentage decreased with increasing concentrations of the ZnO ENM. At 20, 50 and 100 µg/mL a statistically significant decreased in viability was seen, as compared to the negative control.

This project has received funding from the European Union's Horizon 2020 research and innovation programme under grant agreement No 814425.

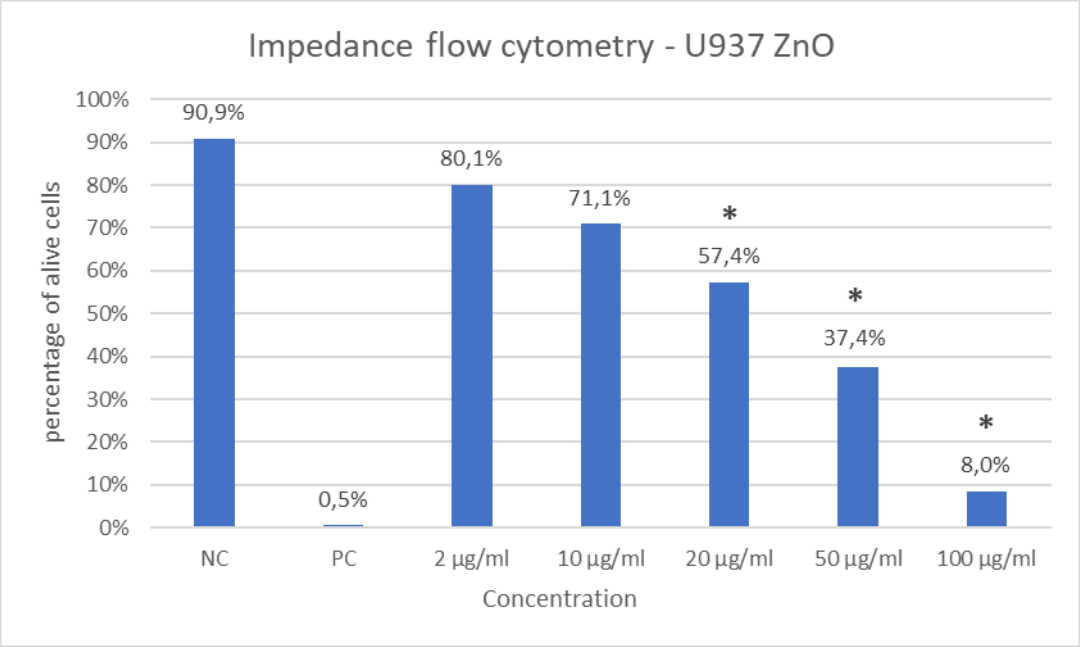

Fig. 20. Percentage of viable U937 cells following exposure for 24 h to ZnO at different concentrations (2, 10, 20, 50 and 100 µg/mL). NC = negative control, PC = Positive control. Complete DMEM (10% FBS) was used for the cells. Cells were seeded at 100 000 cells/mL. "*" marked statistical significance compared to the control, $p < 0.05$ (One-way Anova).

4.4 Impedance-based measurements using a microfluidic system

After assessing the toxic effects under static exposure conditions, the next step was to develop and assess the same toxicity parameters in a 2D biological model in a dynamic environment, i.e., constant perfusion of nutrients and homogenous ENM dispersions. The intention was to develop a dynamic environment that mimics *in vivo* microvascular channels. First, the optimal cell ratio and surface coating for growing ZF4-cells under dynamic conditions were determined.

4.4.1 Fabrication of the microfluidic chip

The fabrication of the hard mold (SI-master) utilizing photolithography made it possible to cast a PDMS inside a Teflon base polycarbonate lid. The casted PDMS was thereby fused together with a glass coverslip containing a microelectrode array, creating the microfluidic chip featured with microelectrodes (Figure 21). The channels were then coated with PLL (0.02% w/v) and extracellular matrix proteins to seed the ZF4-cells.

This project has received funding from the European Union's Horizon 2020 research and innovation programme under grant agreement No 814425.

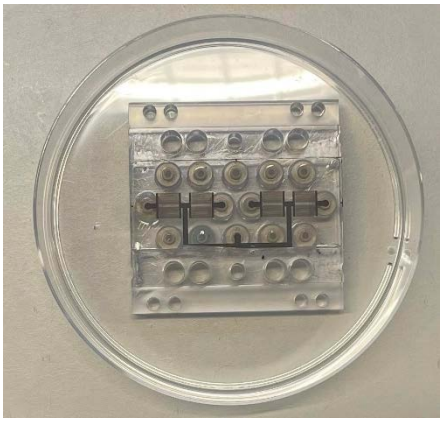

Fig. 21. Fabricated microfluidic chip featured with microvascular channels and a glass coverslip containing microelectrode array inside a petri dish.

4.4.2 Determination of chip conditions and optimization

The optimal coating of the microfluidic channels for growing ZF4 cells was determined by coating three channels with PLL (0.02% w/v), PLL (0.02% w/v) + laminin (50 µg/mL) and PLL (0.02% w/v) + fibronectin (50 µg/mL). Figure 22 shows the microfluidic channels coated with PLL (0.02% w/v), PLL (0.02% w/v) + laminin (50 µg/mL) and PLL (0.02% w/v) + fibronectin (50 µg/mL). To decide which coating to use, the time it took for the cells to adhere was important. The PLL coated channel captured a high number of cells, but it took cells about 2 h to start expanding as seen in Figure 22. Cells seeded on PLL + fibronectin also did not adhere straight away, adhesion started around 1 h. PLL + Laminin showed a high number of cells capture and fast cell body expansion within 0.5 h. In addition, by the end of culture time (24 h), ZF4 cells culture on PLL + laminin formed denser and more continuous monolayer than cell cultures onto the other coatings. Therefore, we then continued with the PLL + Laminin coated channel.

This project has received funding from the European Union's Horizon 2020 research and innovation programme under grant agreement No 814425.

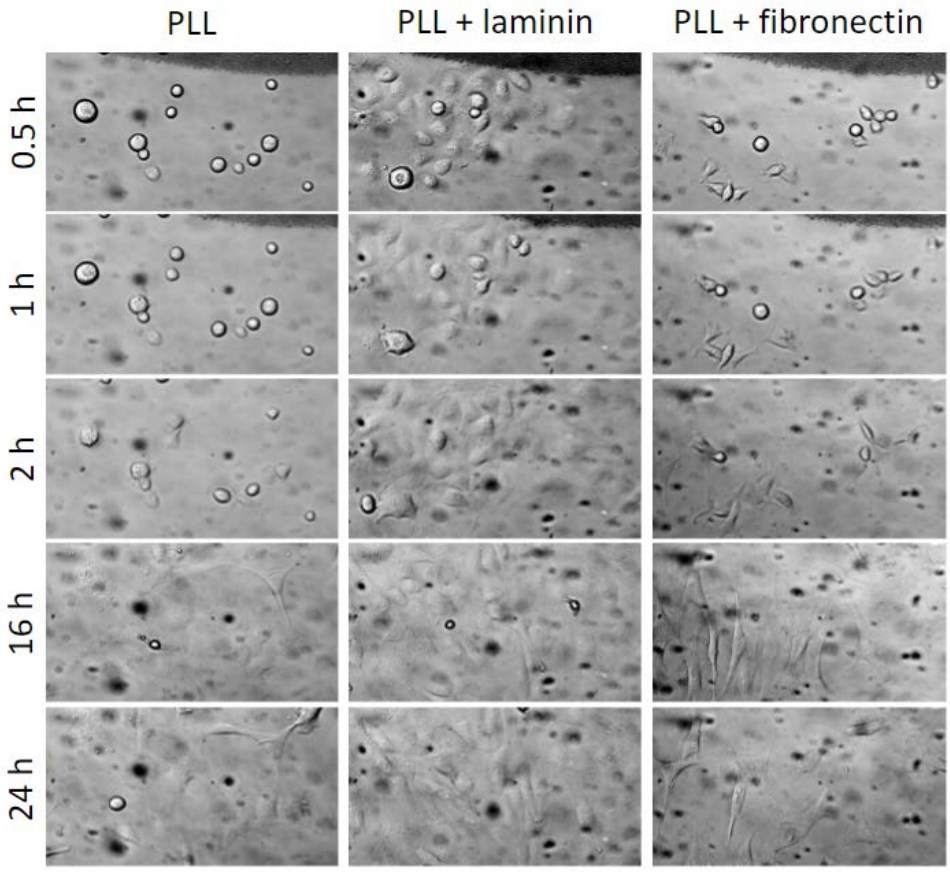

Fig. 22. Imaging of microfluidic chip channels coated with PLL, PLL + laminin, PLL + fibronectin. 0.5, 1, 2, 16 and 24 h after ZF4 cells seeding.

To determine the flow of the fluid in the microfluidic channels, multiple flow speeds were tested. Figure 23 shows the different flow velocities that the cells were exposed to: 5 µl/min, 8 µl/min and 22 µl/min for 24 h. Both the 5 and 8 µl/min did not show much difference throughout the 24 h, while the 22 µl/min had a stronger effect on the ZF4 cells, which appeared less well attached (rounder) at 8 h and towards the end of the cell culture. The 22 µl/min appeared to be too strong for the cells, which started to lift and die. Therefore, we chose to proceed using a fluid velocity of 15 µl/min.

This project has received funding from the European Union's Horizon 2020 research and innovation programme under grant agreement No 814425.

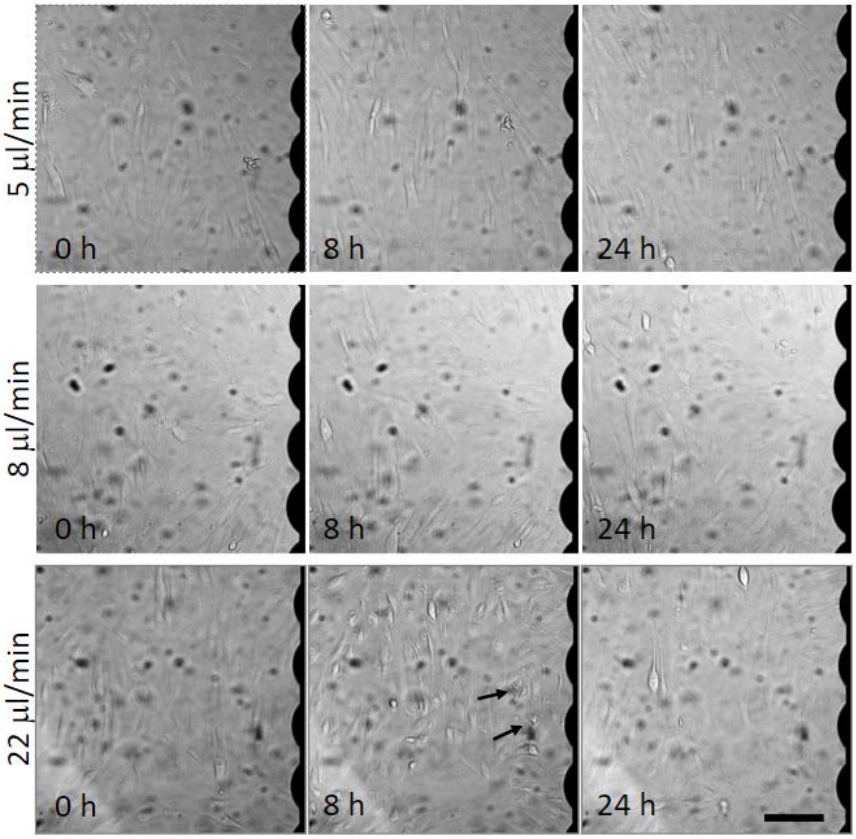

Fig. 23. Imaging of ZF4-cells under 5, 8 and 22 µl/min flowrates at 0 h, 8 h and 24 h. The flowrate of 22 µl/min had a negative effect on cell density and viability from the 8 h to 24 h imaging.

After finding the appropriate conditions for culturing ZF4 cells in the microfluidic chip, we monitored the electrical impedance to follow cell growth. The cells were monitored after seeding ($2x10^6$ cell/mL) (Figure 24). The cells grew normally for the initial 20 h. The impedance reading in Figure 25 shows an initial jump, which indicates the addition of cells. The impedance readings continue to increase, which was expected due to cell body expansion and proliferation of the cells in the channel. At the 20 h mark, fresh cell culture medium was added, which is indicated by the jump in impedance. From 20 h to 40 h, the impedance dropped and from the imaging it is possible to see that the cells start to bundle and lose contact to the substrate. At 25-30 h the cells started to lift off from the surface, suggesting disruption of cell-substrate interaction mediated by the shear stress and high cell number.

This project has received funding from the European Union's Horizon 2020 research and innovation programme under grant agreement No 814425.

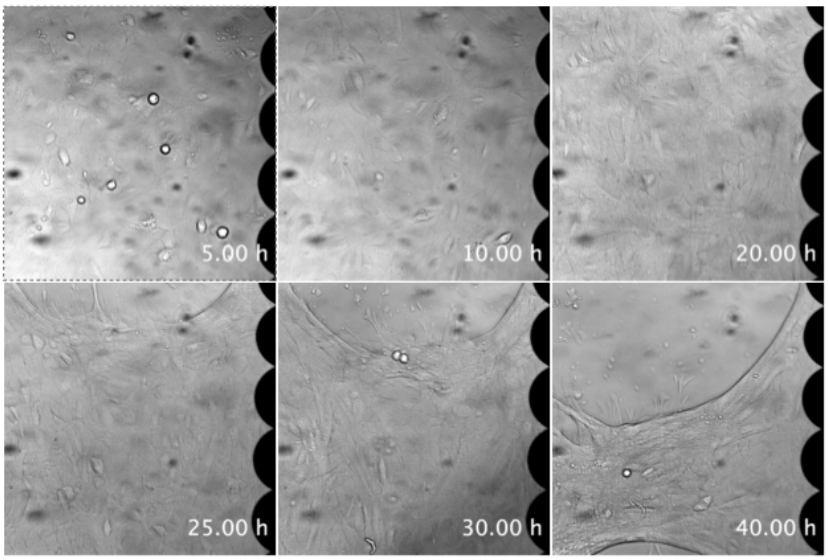

Fig. 24. ZF4-cells in the microfluidic channel at a flowrate of 15 ul/min. Imaging taken over a 40 h timespan.

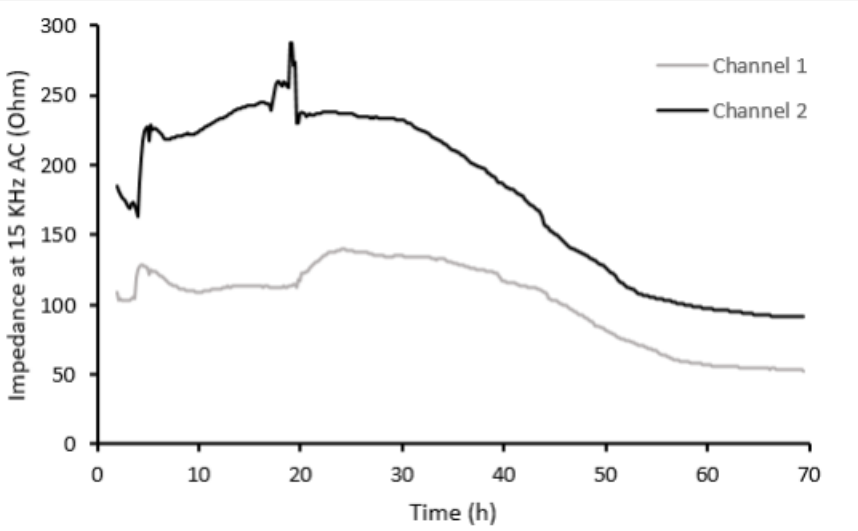

Fig. 25. Impedance-based readings in two microfluidic channels with ZF4 cells. Two separate channels. Channel 1 contained considerably less cells than channel 2. Note the initial jump in impedance due to addition of cells. Spike in impedance at 20 h due to addition of new cell culture medium.

To combat bubble formation, bubble traps were introduced to the system (Figure 26), which has also been done previously (Skelley & Voldman 2008). The bubble traps worked, and bubbles did not interfere with the experiment anymore (Fig. 25).

This project has received funding from the European Union's Horizon 2020 research and innovation programme under grant agreement No 814425.

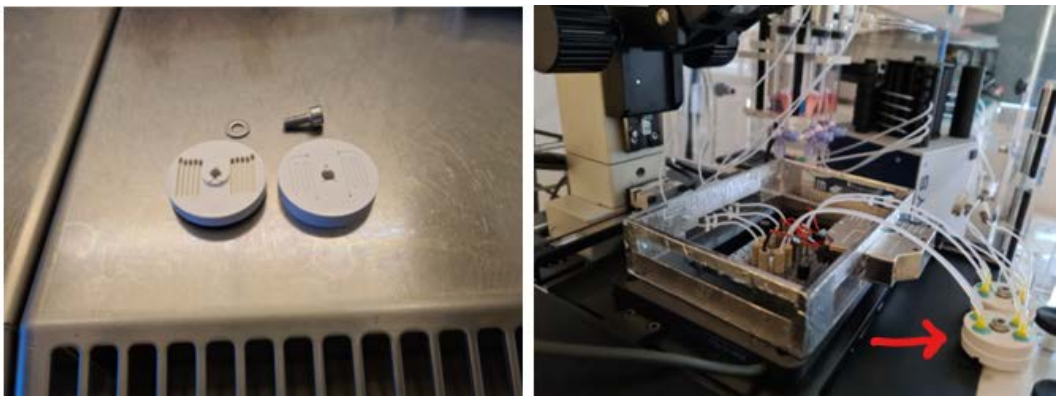

Fig. 26. B*ubble traps (Left) and bubble traps connected to the microfluidic system (Right).*

4.5 Comparison of cell line sensitivity

To assess the sensitivity of the fish cell types, the response of RTgut and ZF4 cells to the selected ENMs was compared. Furthermore, the responses of the above mentioned fish cells were compared with that of the human A549 cells. The human cell line A549 is an immortalized human lung adenocarcinoma epithelial cell line and several nano-toxicity studies have been carried out using this cell line (Foster et al. 1998, Martin et al. 2017). The Rtgut is an intestinal epithelial cell line proposed as equivalent to the Caco-2 cell line for human intestinal epithelium (Kawano et al. 2011). It is a well characterized cell line which improves environmental monitoring of potential ENM toxic effects (Minghetti & Schirmer 2016, Antony Jesu Prabu et al. 2018). The ZF4 cells are a type of fibroblast cells, established from 1-day old zebrafish embryos. The Organization for Economic Cooperation and Development (OECD) has acknowledged zebrafish as one of the regulatory test species, with several representative stages frequently utilized for toxicity testing, such as zebrafish embryos for assessing acute toxicity (OECD 2013, OECD 2014). The use of these fish cells broadens the toxicological hazard assessment towards environmental concerns, and the work presented here also extends the applicability of OECD TG 249 on Rainbow Trout gill cells.

Based on the results obtained, the calculated EC_{50} values (Table 4), and the results of the modeling that considers the kinetics of the cellular response (Figure 27), ZF4 cells were the ones on which the ENMs had the greatest effect and are therefore the most sensitive cell line. The cell line that showed the most resilience was the RTgut. This indicates a clear distinction between the tissues from which each cell line is derived, and is aligned with the life stages (i.e., embryo cells being especially sensitive) and function (i.e., the gut barrier cells being resilient to challenge). The RTgut reflects the mature fish intestine, which is a multifunctional resilient organ responsible for processes such as digestion, adsorption of nutrients and osmoregulation (Kiron et al. 2012, Wang et al. 2019), while the ZF4 is an embryonic early stage ecotoxicological model, which enables them to be used as an additional model in the study of acute toxicity fish test (Yang et al. 2009, Quevedo et al. 2021). The A549 cells were more resilient, which is in line with studies that have reported that cancer cells were less sensitive to ENMs and more resistant to toxic effects than normal cells (Chang et al. 2007).

This project has received funding from the European Union's Horizon 2020 research and innovation programme under grant agreement No 814425.

The toxicity assessment using the derivative of FC vs. control in impedance-based measurements obtained with the xCELLIgence system (Matlab) is presented in Figure 27.

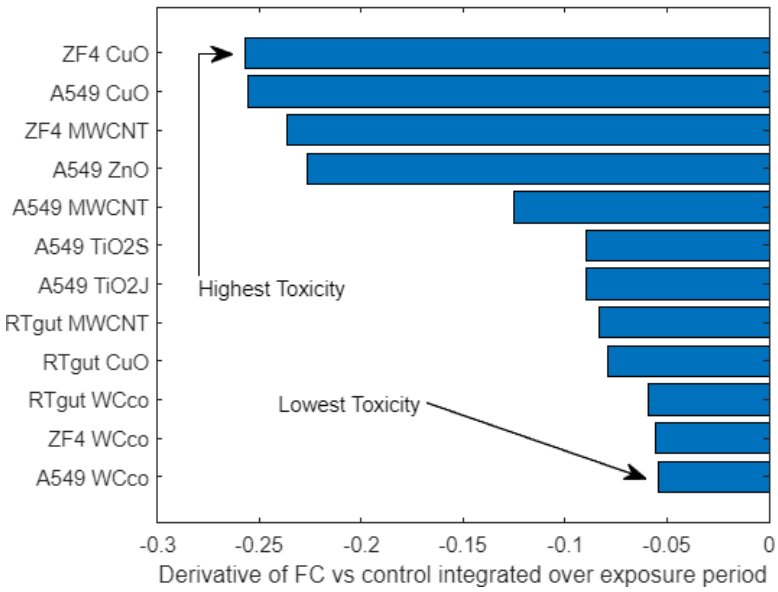

Fig. 27. Toxicity evaluation using the derivative of FC vs. control in impedance-based measurements obtained with the xCELLIgence system. ZF4, RTgut and A549 cells exposed to ENMs at 100 ug/ml for 24 h.

Table 4: EC_{50} values for each ENM in RTgut, ZF4, and A549 cells.

Nanomaterials	RTgut cells	ZF4 cells	A549 cells
	EC_{50} [µg/mL]		
CuO	92.66	15.32	38.13
WC-co	N. R	N. R	N. R
MWCNT	> 100	2.5	> 100
Dispersant (MWCNT)	97.7	3.1	91.7

EC_{50} is the half maximal effective concentration of a substance, thus indicating the potency of the respective substances. N.R means the value is not reached for the concentrations tested.

The RTgut, ZF4, and A549 are distinct cells derived from the intestine, embryo, and lung, respectively. When the three cell lines are compared, ZF4 is the most sensitive, whereas RTgut and A549 respond similarly to the different ENMs. There is a quick reaction of the ZF4 cells to ENMs. Furthermore, the reaction is severe resulting in very low NCI values, indicating cell death. The real-time measurements of the RTgut cells were different from ZF4 and A549. Before the addition of ENMs there was a proliferation of cells which stagnated before it proliferated again. The addition of ENMs did not necessarily have an

This project has received funding from the European Union's Horizon 2020 research and innovation programme under grant agreement No 814425.

initial negative effect. For many ENM concentrations, proliferation was seen in the beginning. This proliferation did however come to an end, and for some of the highest exposure concentrations the drop was significant. The A549 cells proliferated in a linear manner and when exposed to ENMs there was a small reaction with a more marked decrease for ZnO and CuO.

4.6. Static vs dynamic exposure conditions

One of the aims of this research was to compare the effects of ENM exposure under static and dynamic exposure conditions on ZF4-cells. This was however not yet finalized due to unpredicted problems (damage of the cell lines container), Covid 19 pandemic, and moving of the microfluidic system from its previous location at another Institute.

The development and construction of a microfluidic chip for ZF4 exposure to well-defined flows of ENMs was accomplished. The identification of the optimal electrode coating and flow rate to investigate the ZF4-cells behavior in the manufactured microfluidic channels were also accomplished. Work is in progress to assess the effects of selected ENMs on a new set of ZF4 cells received from UoB.

4.7. Effect of conditioning on daphnia longevity

D. magna prefers living in groups, the communication within which is believed to be governed by the release of kairomones. Since the miniaturisation assay also considers the daphnids being placed individually into wells of the multi-well plates, we investigated the impact of this on the daphnia lifetime and overall fitness. Thus, in order to highlight the importance of the *D. magna* medium conditioning for the organisms themselves (as well as for the ENM eco-corona formation), and as a basis on which to build the subsequent miniaturisation study, an assessment of the impact of conditioning media on daphnia longevity was performed, to assess the impact of kairomone governed population regulation was conducted. Figure 28 shows that *D. magna* grouped together survived for the longest duration, reducing to 50% survivorship at approximately 85 days and with the last organism mortality occurring at 120 days, compared to single neonates in plain medium reaching just 50% survivorship at approximately 65 days and the last neonate mortality occurring before 90 days. Interestingly, the single neonates exposed to conditioned medium (containing kairomones previously released by *D. magna*) had a much higher survival rate than the isolated organisms in plain medium, maintaining 50% survivorship past 70 days with the last organism mortality occurring past 110 days, results which are similar to those of the neonates that had been grouped together (Figure 28), indicating the importance of secreted biomolecules to organism health.

This increased survivorship of single *D. magna* in conditioned medium (previously inhabited by other *D. magna*) compared to single neonates in plain medium is likely due to the presence of kairomone secretions by previous *D. magna* into the running culture medium used for the growth phase (Nasser et al., 2020). *D. magna* communicates through kairomone secretion as the level of kairomones dictates population survival, for example, when numbers of *D. magna* are too high which may lead to lack of resources such as food, it promotes death in the culture. Alternatively, when kairomone levels are too low and the population is at risk of survival, it promotes a stress response to switch to sexual reproduction leading to production of diapause eggs to ensure the future survival of the population as

This project has received funding from the European Union's Horizon 2020 research and innovation programme under grant agreement No 814425.

the current population dies out. Single females exposed to medium having previously contained a healthy population size and thus a suspected healthy level of kairomones survive significantly better than single females exposed to control medium. This data is important as it shows that *D. magna* secretes biomolecules other than the already well-established proteins and carbohydrates, which will inevitably compete for space at the NMs surface to form part of the NMs corona, which may also influence toxicity tests by reducing the concentration of these key biomolecules that promote survivorship. These data also support the need for medium conditioning to be added to standardized OECD ecotoxicity tests relating to *D. magna*, as the absence of kairomones may make the test organisms generally less robust, and thus more susceptible to toxicants.

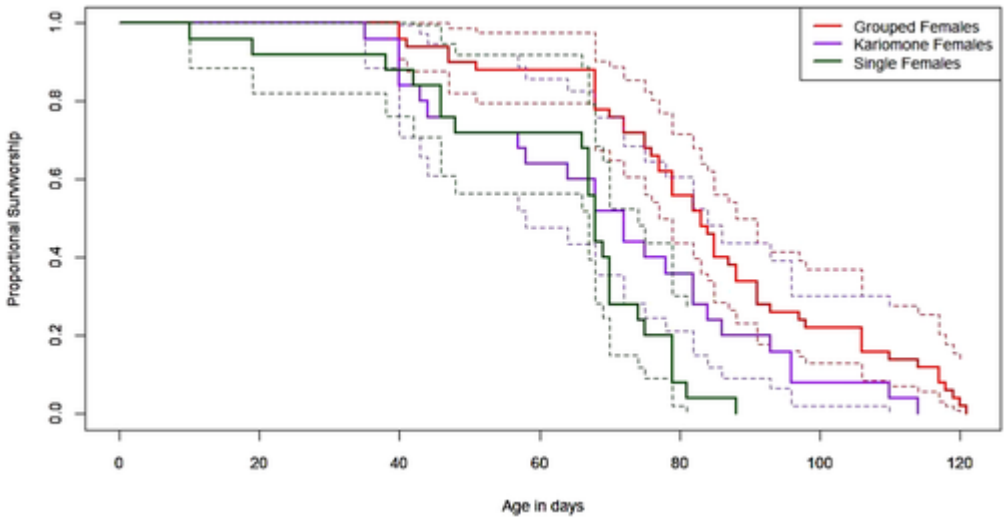

Fig. 28. Survivorship of five grouped females (red), single females in plain medium (green) and single neonates in medium conditioned by previously containing 20 females (15–20 days old) (purple). Dotted lines represent Kaplan–Meier 95% confidence markers (*n* = 25 in each group). From Nasser et al., 2020.

Analysis of the miniaturization results is underway and these will be reported in the final report, and a dedicated publication to ensure maximum impact. Ongoing work is to extend the assay to consider reproduction also, especially now that we have shown that we can reduce the impacts of culturing daphnids individually through use of daphnia-conditioned medium. This is especially exciting as both growth and reproduction data are needed as input data to feed into the Dynamic Energy Budget model that is being integrated into the Impaired Daphnia Reproduction Adverse Outcome Pathway, which was described in outline in Deliverable Report D6.4 (Report on (feedback on) initial DEB-based AOP for chronic ecotoxicity to ENMs (based on workshop)) and which is further updated and a more complete dataset included in Deliverable Report D6.5 (Report on DEB-based AOP for chronic ecotoxicity to ENMs, and extension to multi-generational effects) from RiskGONE.

This project has received funding from the European Union's Horizon 2020 research and innovation programme under grant agreement No 814425.

5. Conclusions

In Task 6.2, we have refined and finalised *in vitro* assays for nanosafety eco-toxicological hazard assessment based on RT gut and ZF4 cells (UiB and UoB) and a miniaturised multi-well assay for *D. magna* growth (UoB), using conditions that are more relevant for *in vivo* exposure to ENMs.

High-throughput impedance-methods were implemented with the aim to provide a set of reliable, cost- and time-efficient methods for nanotoxicity screening and SOPs were established.

Cyclic voltammetry, an electrochemical method, was to our knowledge adapted for the first time for the assessment of ENM-induced oxidative stress in a label-free manner and a mathematical model to interpret the results was developed. Cyclic voltammetry was developed in WP5 on human cells and will also be implemented for fish cells.

The xCELLigence system was used to examine the putative toxic effect on fish RTgut and ZF4 as well as human A549 cells exposed to a series of ENMs under static exposure conditions using real-time impedance measurements. A mathematical model was developed, which takes into consideration the kinetics of the cellular response. The CuO, ZnO and MWCNT ENMs induced the highest cytotoxicity followed by WC-co. The ZF4 cellular model proved to be the most sensitive followed by A549 and RTgut, indicating that the human or fish origin did not play a significant role, and that the assay is widely applicable.

To evaluate in real-time the effect of ENMs on ZF4 cells under dynamic exposure conditions a microfluidic system was designed and constructed. The development and construction of a microfluidic chip for ZF4 exposure to well-defined flows of ENMs was accomplished. The identification of the optimal electrode coating and flow rate to investigate the ZF4-cells behavior in the manufactured microfluidic channels were also accomplished.

One of the main sources of uncertainties in nanotoxicity assessment is represented by ENM interferences with testing systems. Impedance-based methods are label-free and thus, less prone to possible ENM-induced interferences. Since no chemical reagents are needed, such methods are also more eco-friendly. Another important advantage is that cells can be monitored in real-time, which allows the identification of relevant concentrations and timepoints for further in-depth mechanistic studies. Impedance-based monitoring gives information regarding cell proliferation, adhesion and viability and by coupling it with live microscopy, more information on cells' behaviour during ENM exposure can be obtained. Impedance-based methods emerge as effective, environmentally friendly, and reliable, especially as a first-line screening tool to assess the cellular viability after ENM exposure.

The efforts towards miniaturisation of the daphnia assays for immobilisation and especially for growth which is a choric assay over 21 days and is an integral aspect of the reproduction assay are important, and the key role of pre-conditioning the medium by multiple daphnids in order to provide the signalling background and community "feel" that promotes daphnia longevity and fitness was revealed, which reduced potential concerns of regulators related to culturing daphnids singly over extended periods.

The data obtained, the methods and the biological models are also feeding into NanoHarmony for further evaluation and inter-laboratory comparisons, to support the activities of the OECD WPMN and other standardization bodies. This activity forms the basis of SOPs to be taken forward as guidance documents to ensure the translation of the scientific data generated into risk management tools underpinning an ERA framework, and is an enduring and important outcome from the RiskGONE project.

This project has received funding from the European Union's Horizon 2020 research and innovation programme under grant agreement No 814425.

6. References

Antony Jesu Prabhu, P., et al., Zinc uptake in fish intestinal epithelial model RTgutGC: Impact of media ion composition and methionine chelation. Journal of Trace Elements in Medicine and Biology, (2018) 50: 377-383.

Ceriotti, L., et al. Assessment of cytotoxicity by impedance spectroscopy. Biosens Bioelectron (2007) 22: 3057-3063.

Chang, J.-S., et al., In Vitro Cytotoxicitiy of Silica Nanoparticles at High Concentrations Strongly Depends on the Metabolic Activity Type of the Cell Line. Environmental Science & Technology, (2007) 41(6): 2064-2068.

Chetwynd, A.J., Lynch, I. The rise of the nanomaterial metabolite corona, and emergence of the complete corona. Environmental Science: Nano, (2020) 7, 1041-1060.

Chevion, S., et al., Evaluation of Plasma Low Molecular Weight Antioxidant Capacity by Cyclic Voltammetry. Free Radical Biology and Medicine (1997) 22(3): 411-421.

Chevion, S., et al., Antioxidant Capacity of Edible Plants: Extraction Protocol and Direct Evaluation by Cyclic Voltammetry. Journal of Medicinal Food (1999) 2(1): 1-10.

Chevion, S., et al. The use of cyclic voltammetry for the evaluation of antioxidant capacity. Free Radic Biol Med (2000) 28(6): 860-70.

Collins, A. R., *et al*. High throughput toxicity screening and intracellular detection of nanomaterials. *Wiley Interdiscip. Rev. Nanomedicine Nanobiotechnology* (2016) 9, e1413.

DeLoid, G.M., et al., Preparation, characterization, and in vitro dosimetry of dispersed, engineered nanomaterials. Nat Protoc (2017). 12(2): 355-371.

Drasler, B.; et al. In vitro approaches to assess the hazard of nanomaterials. NanoImpact (2017) 8: 99-116. https://doi.org/10.1016/j.impact.2017.08.002.

Cimpan, M. R., et al. An impedance-based high-throughput method for evaluating the cytotoxicity of nanoparticles. *J. Phys.: Conf. Ser.* (2013) 429 012026. DOI 10.1088/1742-6596/429/1/012026.Dusinska, M., et al. Towards an alternative testing strategy for nanomaterials used in nanomedicine: lessons from NanoTEST. Nanotoxicology (2015), 9 Suppl 1: 118-132.

Elgrishi, N., et al., A Practical Beginner's Guide to Cyclic Voltammetry. Journal of Chemical Education (2018) 95(2): 197-206.

Fadeel., B., et al. Advanced tools for the safety assessment of nanomaterials. Nat Nanotechnol. (2018) 13(7): 537-543. doi: 10.1038/s41565-018-0185-0.

Foster, K.A., et al., Characterization of the A549 Cell Line as a Type II Pulmonary Epithelial Cell Model for Drug Metabolism. Experimental Cell Research, 1998. 243(2): p. 359-366.

Guadagnini, R., et al. Toxicity screenings of nanomaterials: challenges due to interference with assay processes and components of classic in vitro tests. Nanotoxicology (2015) 9 Suppl 1: 13-24.

Grintzalis, K., Dai, W., Panagiotidis, K., Belavgeni, A., Viant, M.R. Miniaturising acute toxicity and feeding rate measurements in Daphnia magna. Ecotoxicology and Environmental Safety, 2017, 139: 352-357.

This project has received funding from the European Union's Horizon 2020 research and innovation programme under grant agreement No 814425.

Hondroulis, E., et al. Whole cell based electrical impedance sensing approach for a rapid nanotoxicity assay. Nanotechnology (2010) 21: 315103

Jensen, A. K. NANoREG D2.08 SOP 02 for measurement of hydrodynamic Size-Distribution and Dispersion Stability by DLS, (2017) https://www.rivm.nl/sites/default/files/2018-11/NANoREG%20D2.08%20SOP%2002%20For%20measurement%20of%20hydrodynamic%20Size-Distribution%20and%20Dispersion%20Stability%20by%20DLS.pdf.

Kawano, A., et al., Development of a rainbow trout intestinal epithelial cell line and its response to lipopolysaccharide. Aquaculture Nutrition (2011) 17(2): E241-E252.

Kiron, V., Fish immune system and its nutritional modulation for preventive health care. Animal Feed Science and Technology (2012) 173(1): 111-133.

Kroll, A., et al. Interference of engineered nanoparticles with in vitro toxicity assays. Arch Toxicol (2012) 86: 1123-1136.

Lynch, I., Dawosn, K.A. Lead, J.R., Valsmai-Jones, E. Macromolecular Coronas and their Importance in Nanotoxicology and Nanoecotoxicology, Frontiers of Nanoscience. Elsevier, Amsterdam 2014.

Martin, A. and A. Sarkar, Overview on biological implications of metal oxide nanoparticle exposure to human alveolar A549 cell line. Nanotoxicology (2017) 11(6): 713-724.

Minghetti, M., and Schirmer. K., Effect of media composition on bioavailability and toxicity of silver and silver nanoparticles in fish intestinal cells (RTgutGC). Nanotoxicology (2016) 10(10): 1526-1534.

Nasser, F., Constantinou, J., Lynch I. Nanomaterials in the Environment Acquire an “Eco-Corona” Impacting their Toxicity to Daphnia Magna—a Call for Updating Toxicity Testing Policies. Proteomics, 2020, 20 (9), 1800412.

OECD, Test No. 236: Fish Embryo Acute Toxicity (FET) Test. 2013.

OECD, Fish Toxicity Testing Framework. 2014.

Ostermann, M., et al. Label-free impedance flow cytometry for nanotoxicity screening. Sci Rep (2020) 10, 142. https://doi.org/10.1038/s41598-019-56705-3.

Pliquett, U. Bioimpedance: A Review for Food Processing. Food Engineering Reviews (2010) 2: 74-94.

Prodan, E., et al. The Dielectric Response of Spherical Live Cells in Suspension: An Analytic Solution. Biophysical Journal (2008) 95: 4174-4182.

Psotová, J., et al., Determination of total antioxidant capacity in plasma by cyclic voltammetry. Two case reports. Biomedical Papers (2001) 145(2): 81-83.Seiffert, J. M., et al. Dynamic monitoring of metal oxide nanoparticle toxicity by label free impedance sensing. Chem Res Toxicol (2012) 25(1): 140–152.

Quevedo, C., et al. Silver nanoparticle induced toxicity and cell death mechanisms in embryonic zebrafish cells. Nanoscale (2021). 13. 6142-6161

Ruzycka, M., et al. Microfluidics for studying metastatic patterns of lung cancer. J Nanobiotechnol (2019) 17: 71. https://doi.org/10.1186/s12951-019-0492-0.

Schwan, H. P., & KAY, C. F. The conductivity of living tissues. Annals of the New York Academy of Sciences (1957) 65: 1007-1013.

This project has received funding from the European Union’s Horizon 2020 research and innovation programme under grant agreement No 814425.

Skelley, A.M. and J. Voldman, An active bubble trap and debubbler for microfluidic systems. Lab on a Chip. (2008) 8(10): 1733-1737.

Vinkovic Vrcek, I., *et al*. Does surface coating of metallic nanoparticles modulate their interference with *in vitro* assays? RSC Adv. (2015) 5: 70787–70807.

Wang, J., et al., Rainbow Trout (Oncorhynchus Mykiss) Intestinal Epithelial Cells as a Model for Studying Gut Immune Function and Effects of Functional Feed Ingredients. Frontiers in Immunology (2019) 6;10:152. doi: 10.3389/fimmu.2019.00152.

Wu, H., Gonzalez-Pech, N.I., Grassian, V.H. Displacement reactions between environmentally and biologically relevant ligands on TiO2 nanoparticles: insights into the aging of nanoparticles in the environment. Environ. Sci.: Nano, 2019, 6, 489-504.

This project has received funding from the European Union's Horizon 2020 research and innovation programme under grant agreement No 814425.

www.riskgone.eu | riskgone@nilu.no

Bergen, 12 04 2023

This project has received funding from the European Union's Horizon 2020 research and innovation programme under grant agreement No 814425.